UNCLASSIFIED

ERDA Mathematics and Computing Laboratory

Courant Institute of Mathematical Sciences
New York University

Mathematics and Computing COO-3077-145

A SURVEY OF NUMERICAL METHODS FOR COMPRESSIBLE FLUIDS

Gary A. Sod

June 1977

Contract No. EY-76-C-02-3077

UNCLASSIFIED

DISCLAIMER

Abstract

The finite difference methods of Godunov, Hyman, Lax-Wendroff (two-step), MacCormack, Rusanov, the upwind scheme, the hybrid scheme of Harten and Zwas, the antidiffusion method of Boris and Book, and the artificial compression method of Harten are compared with the random choice method known as Glimm's method. The methods are used to integrate the one-dimensional equations of gas dynamics for an inviscid fluid. The results are compared and demonstrate that Glimm's method has several advantages.

I. Introduction

In the past few years many finite difference schemes have been used for solving the one-dimensional equations of gas dynamics for an inviscid fluid. Recently the random choice method (Glimm's method) introduced by Glimm [6], has been developed for hydrodynamics by Chorin [3]. Due to the nonstandardness of Glimm's method, as well as the difficulty in programming, its acceptance as an effective and efficient numerical tool may be restricted.

In the following sections a brief discussion of the methods is given, their solution to a sample one-dimensional problem is compared, the advantages of Glimm's method are discussed, and finally the equations used by Glimm's method are derived and a flow chart for the programming of it is given.

Basic Equations. The one-dimensional equations of gas dynamics may be written in the (conservation) form:

$$\partial_t \rho + \partial_x(\rho u) = 0 , \tag{1}$$

$$\partial_t m + \partial_x\left(\frac{m^2}{\rho} + p\right) = 0 , \tag{2}$$

$$\partial_t e + \partial_x\left(\frac{m}{\rho}(e+p)\right) = 0 \tag{3}$$

where ρ is the density, u is the velocity, $m = \rho u$ is momentum, p is pressure, and e is energy per unit volume. We may write $e = \rho\varepsilon + \frac{1}{2}\rho u^2$, where ε is the internal energy per unit mass. Assume the gas is polytropic, in which case

$$\varepsilon = \frac{p}{(\gamma-1)\rho} \tag{4a}$$

where γ is a constant greater than one. Furthermore, from (4a) we have

$$p = A(S)\rho^{\gamma} \tag{4b}$$

where S denotes entropy.

Equations (1)-(3) may be written in vector form

$$\underline{U}_t + \underline{F}(\underline{U})_x = 0 \tag{5}$$

where

$$\underline{U} = \begin{pmatrix} \rho \\ m \\ e \end{pmatrix} \quad \text{and} \quad \underline{F}(\underline{U}) = \begin{pmatrix} m \\ \frac{m^2}{\rho} + p \\ \frac{m}{\rho}(e+p) \end{pmatrix} .$$

In order to deal with solutions which contain shocks, we write the equations in integral form, which is obtained by integrating equations (1)-(3) (or equation (5)) over any region in the upper half of the (x,t) plane and applying Green's theorem to obtain the following contour integrals

$$\oint \rho dx + \oint m dt = 0 , \tag{6}$$

$$\oint m dx + \oint (\frac{m^2}{\rho} + p) dt = 0 , \tag{7}$$

$$\oint e dx + \oint (\frac{m}{\rho}(e+p)) dt = 0 . \tag{8}$$

II. Description of the Methods

The methods of Godunov [5], Lax-Wendroff (two-step) [16], MacCormack [18], Rusanov [20], and the upwind difference scheme [19] have been widely used and no benefit can be obtained by describing them here. Hence, these schemes will merely be listed in Table I. The remaining methods under consideration will be briefly discussed.

Glimm's Method. Consider the nonlinear system of equations (5). Divide time into intervals of length Δt and let Δx be the spatial increment. The solution is to be evaluated at time $n\Delta x$, where n is a nonnegative integer at the spatial increments $i\Delta x$, $i = 0, \pm 1, \pm 2, \ldots$ and at time $(n+\frac{1}{2})\Delta t$ at $(i+\frac{1}{2})\Delta x$.

The method is a two-step method. Let $\underline{u}_i^n$ approximate $\underline{U}(i\Delta x, n\Delta t)$ and $\underline{u}_{i+1/2}^{n+1/2}$ approximate $\underline{U}((i+1/2)\Delta x,(n+1/2)\Delta t)$. To find the solution $\underline{u}_{i+1/2}^{n+1/2}$ and thus define the method, consider the system (5) along with the piecewise constant initial data

$$\underline{U}(x,n\Delta t) = \begin{cases} \underline{u}_{i+1}^n , & x \geq (i+1/2)\Delta x , \\ \underline{u}_i^n , & x < (i+1/2)\Delta x . \end{cases} \tag{9}$$

This defines a sequence of Riemann problems. If $\Delta t < \frac{\Delta x}{2(|u|+c)}$, where c is the local sound speed, the waves generated by the different Riemann problems will not interact. Hence the solution $\underline{v}(x,t)$ to the Riemann problem can be combined into a single exact solution. Let ξ_n be an equidistributed random variable which is given by the Lebesgue measure on the interval $[-\frac{1}{2},\frac{1}{2}]$. Define

$$\underline{u}_{i+1/2}^{n+1/2} = \underline{v}((i+\xi_n)\Delta x,(n+\tfrac{1}{2})\Delta t). \tag{10}$$

At each time step, the solution is approximated by a piecewise constant function. The solution is then advanced in time exactly and the new values are sampled. The method depends on the possibility of solving the Riemann problem exactly and inexpensively.

Chorin [3] (see also Sod [21]) modified an iterative method due to Godunov [4] which will be described below.

Consider the system (5) with the initial data

$$\underline{U}(x,0) = \begin{cases} S_\ell = (\rho_\ell, u_\ell, p_\ell) , & x < 0 , \\ S_r = (\rho_r, u_r, p_r) , & x \geq 0 . \end{cases} \tag{11}$$

The solution at later times looks like (see [14]) Fig. 1, where S_1 and S_2 are either a shock or a centered rarefaction wave. The region S_* is a steady state. The lines ℓ_1 and ℓ_2 are slip lines separating the states. The slip line $dx/dt = u_*$ separates the state S_* into two parts with possibly different values of ρ_*, but equal values of u_* and p_*.

Using this iterative method we first evaluate p_* in the state S_*. Define the quantity

$$M_\ell = \frac{p_\ell - p_*}{u_\ell - u_*} . \tag{12}$$

If the left wave is a shock, using the jump condition $U_\ell[\rho] = [\rho u]$, we obtain

$$M_\ell = \rho_\ell(u_\ell - U_\ell) = \rho_*(u_* - U_\ell) \tag{13}$$

where U_ℓ is the velocity of the left shock and ρ_* is the density in the portion of S_* adjoining the left shock. Similarly, define the quantity

$$M_r = \frac{p_r - p_*}{u_r - u_*} . \tag{14}$$

If the right wave is a shock, using the jump conditions $U_r[\rho] = [\rho u]$, we obtain

$$M_r = -\rho_r(u_r - U_r) = -\rho_*(u_* - U_r) \tag{15}$$

where U_r is the velocity of the right shock and ρ_* is the density in the portion of S_* adjoining the right shock.

In either of the two cases ((12) or (13) for M_ℓ and (14) and (15) for M_r) we obtain

$$M_r = \sqrt{\rho_r p_r}\ \phi(p_*/p_r)\ , \tag{16a}$$

$$M_\ell = \sqrt{\rho_\ell p_\ell}\ \phi(p_*/p_\ell) \tag{16b}$$

where

$$\phi(x) = \begin{cases} \sqrt{\frac{\gamma+1}{2}\,x + \frac{\gamma-1}{2}}\ , & x \geq 1\ , \\ \frac{\gamma-1}{2\sqrt{\gamma}}\,\frac{1-x}{1-x^{\gamma-1/2\gamma}}\ , & x \leq 1\ . \end{cases} \tag{17}$$

Upon elimination of u_* from (12) and (14) we obtain

$$p_* = \frac{(u_\ell - u_r + \frac{p_r}{M_r} + \frac{p_\ell}{M_\ell})}{\frac{1}{M_\ell} + \frac{1}{M_r}}\ . \tag{18}$$

Equations (16a), (16b), and (18) represent three equations in three unknowns for which it can be seen that there exists a real solution. Upon choosing a starting value p_*^o (or M_ℓ^o and M_r^o), we iterate using equations (16a), (16b), and (18). For details of the starting values see Chorin [3] and Sod [21].

After p_*, M_ℓ, and M_r have been determined we may obtain u_* by eliminating p_* from equations (12) and (14),

$$u_* = \frac{p_\ell - p_r + M_\ell u_\ell + M_r u_r}{M_\ell + M_r} . \tag{19}$$

The finite difference method due to Godunov [5] in Table I is for the Eulerian form of the equations of gas dynamics. The method developed by Godunov [4] for the Lagrangian form is also a two-step method where the second step is the second half step in Table I. However, the values of $u_{i+1/2}^{n+1/2}$ and $p_{i+1/2}^{n+1/2}$ are replaced by u_* (19) and p_* (18) from the Riemann problem at i+1/2.

Artificial Viscosity. In the methods of Godunov, MacCormack, and Lax-Wendroff (two-step) an artificial viscosity term was added. The artificial viscosity term used was introduced by Lapidus [13]. It has the advantage that it is very easy to add to an existing scheme and it retains the high order accuracy of the scheme. Let $\underset{\sim}{u}_i^{n+1}$ be the approximation at time $(n+1)\Delta t$ obtained by any one of the above schemes. This value is replaced by the new approximation

$$\underline{u}_i^{n+1} = \underset{\sim}{u}_i^{n+1} + \frac{\nu \Delta t}{\Delta x} \Delta' \left[|\Delta' \underset{\sim}{u}_{i+1}^{n+1}| \cdot \Delta' \underline{\underset{\sim}{u}}_{i+1}^{n+1} \right] \tag{20}$$

where $\Delta' \underset{\sim}{u}_i^n = \underset{\sim}{u}_i^n - \underset{\sim}{u}_{i-1}^n$ and ν is an adjustable constant.

This equation (20) is a fractional step for the numerical solution of the following diffusion equation

$$\underline{U}_t = \frac{\nu \Delta t}{\Delta x} (\Delta x^3) [\, |u_x| \underline{U}_x]_x \cdot$$

It is shown (see Ladidus [13]) that this new difference scheme (obtained by adding the artificial viscosity) satisfies the same conservation law that the previous equation did. The values of the constant ν used varied from method to method. This is discussed in the section on numerical results. This artificial viscosity was not added in the smooth regions.

Harten's Corrective Method of Artificial Compression. In this section we discuss the Artificial Compression Method (ACM) developed by Harten [8]. This method is designed to be used in conjunction with an already existing finite difference scheme. The purpose of this method is to sharpen the regions which contain discontinuities whether shocks or contact discontinuities.

Only the basic idea of the ACM will be discussed for the case of a single conservation law. Let $u(x,t)$ be a solution of the conservation law

$$u_t + f(u)_x = 0 \tag{21}$$

which contains a discontinuity $(u_L(t),\ u_R(t),\ S(t))$, where u_L and u_R are the values on the left and right of the jump and S is the speed of the discontinuity. The discontinuity is either a shock or a contact. Assume, without loss of generality that at any given time t the solution u does not take on any values between $u_L(t)$ and $u_R(t)$. Consider the function $g(u,t)$ with properties

$$g(u,t)\ \text{sgn}\ [u_R(t) - u_L(t)] > 0 \quad \text{for} \quad u \in (u_L(t), u_R(t)) , \tag{22}$$

$$g(u,t) \equiv 0 \quad \text{for} \quad u \notin (u_L(t), u_R(t)) . \tag{23}$$

This function g will be called an artificial compression flux.

It can be seen that u is also a solution of the conservation law

$$u_t + (f(u) + g(u,t))_x = 0 \ . \qquad (24)$$

By (23) we see that when u is smooth the equation (24) is identical with equation (21) and the shock speed S(t) remains the same. Finally it is observed (from (22)) that if (u_L, u_R, S) is a shock or contact for equation (21) then it is a shock for the modified equation (24).

The artificial compression method solves the modified equation (24) rather than the original equation (21). For a complete discussion of the implementation of the method see Harten [8].

Let $\underset{\sim}{u}_i^{n+1}$ represent the approximate solution vector to (5) obtained by using any one of the above finite difference methods. In solving the modified system (analogous to (24)) we use operator splitting. We first define the difference representation $\underline{g}_i$ of the artificial compression flux g,

$$\underline{g}_i = \alpha_i \underline{\Delta}_i \ , \qquad (25)$$

where

$$\underline{\Delta}_i = \underset{\sim}{u}_{i+1} - \underset{\sim}{u}_{i-1}$$

and

$$\alpha_i = \max\left\{0, \min_k \left[\frac{\min\left(|\delta^k_{i+1/2}|, \delta^k_{i-1/2} \cdot \operatorname{sgn}\left(\delta^k_{i+1/2}\right)\right)}{|\delta^k_{i+1/2}| + |\delta^k_{i-1/2}|}\right]\right\} \qquad (26)$$

where k refers to the k-th component of the $\underset{\sim}{u}$, $\delta^k_{i+1/2} = \tilde{u}^{(k)}_{i+1} - \tilde{u}^{(k)}_i$.

Let $\underline{S}_{i+1/2}$ represent the vector whose k-th component is sgn $(\delta^k_{i+1/2})$. Then the difference scheme which applies the ACM to the given solution $\underset{\sim}{u}^{n+1}_i$ is

$$\underline{u}_i^{n+1} = \underset{\sim}{u}^{n+1} - \frac{\Delta t}{2\Delta x}(\underline{g}_{i+1} - \underline{g}_{i-1}) + \frac{\Delta t}{2\Delta x}(|\underline{g}_{i+1} - \underline{g}_i|\underline{S}_{i+1/2} - |\underline{g}_i - \underline{g}_{i-1}|\underline{S}_{i-1/2}) \tag{27a}$$

$$= \underset{\sim}{u}_i^{n+1} - \frac{\Delta t}{2\Delta x}(\underline{G}^n_{i+1/2} - \underline{G}^n_{i-1/2}), \tag{27b}$$

where $\underline{G}^n_{i+1/2} = \underline{g}^n_i - \underline{g}^n_{i+1} - |\underline{g}^n_{i+1} - \underline{g}^n_i|\ \underline{S}_{i+1/2}$, applied componentwise. See Harten [7].

The method of artifical compression is designed for first order schemes and cannot be applied directly to higher order schemes. The idea of ACM is based on the existence of a viscous profile. See Harten [8]. Higher order schemes introduce other flux terms so that one obtains different (nonphysical) speeds of propagation.

Self-Adjusting Hybrid Schemes. The idea of self-adjusting hybrid schemes was introduced by Harten and Zwas [11]. Consider a nonoscillatory first order scheme L_1 and a k-th order ($k \geq 2$) scheme L_k,

$$L_1 u_i = u_i - \frac{\Delta t}{\Delta x}(f^1_{i+1/2} - f^1_{i-1/2}), \tag{28}$$

$$L_k u_i = u_i - \frac{\Delta t}{\Delta x}(f^k_{i+1/2} - f^k_{i-1/2}). \tag{29}$$

So as not to violate the conservation, hybridize L_1 and L_k through their numerical fluxes. Define the hybrid operator L by

$$Lu_i = u_i - \frac{\Delta t}{\Delta x}\,(f_{i+1/2} - f_{i-1/2}), \tag{30}$$

where

$$f_{i+1/2} = \theta_{i+1/2}\, f^{1}_{i+1/2} + (1 - \theta_{i+1/2})\, f^{k}_{i+1/2}\,, \tag{31}$$

$\theta_{i+1/2}$ is a scalar quantity (called a switch) which satisfies $0 \le \theta_{i+1/2} \le 1$. At discontinuities the automatic switch is such that $\theta \simeq 1$. Hence at the discontinuities the hybrid scheme is essentially the nonoscillatory first order scheme.

Equation (30) can be written in the form

$$\begin{aligned} Lu_i = L_k u_i + \frac{\Delta t}{\Delta x}\,[&\theta_{i+1/2}\,(f^{1}_{i+1/2} - f^{k}_{i+1/2}) \\ &- \theta_{i-1/2}\,(f^{1}_{i-1/2} - f^{k}_{i-1/2})] \end{aligned} \tag{32}$$

so that if θ is $o(\Delta x^p)$ where the solution is smooth, then for $p \ge k-1$ we have

$$Lu_i = L_k u_i + o(\Delta x^{k+1}). \tag{33}$$

There are many choices for such schemes. The scheme chosen here is discussed in Harten [9]. Taking $k = 2$ we choose MacCormack's scheme and by adding the artificial viscosity term

$$\frac{1}{8}\,(\theta_{i+1/2}\,(u_{i+1} - u_i) - \theta_{i-1/2}\,(u_i - u_{i-1})) \tag{34}$$

to MacCormack's scheme we obtain the first order scheme. The hybridized scheme becomes for the system (5)

$$\underline{U}_i^{\overline{n+1}} = \underline{U}_i^n - \frac{\Delta t}{\Delta x}\left(\underline{F}_{i+1}^n - \underline{F}_i^n\right) \tag{35}$$

$$\underline{U}_i^{n+1} = \frac{1}{2}\left(\underline{U}_i^{\overline{n+1}} - \underline{U}_i^n\right) - \frac{\Delta t}{2\Delta x}\left(\underline{F}_i^{\overline{n+1}} - \underline{F}_{i-1}^{\overline{n+1}}\right)$$
$$+ \frac{1}{8}\left(\theta_{i+1/2}^n\left(\underline{U}_{i+1}^n - \underline{U}_i^n\right) - \theta_{i-1/2}^n\left(\underline{U}_i^n - \underline{U}_{i-1}^n\right)\right). \tag{36}$$

The stability condition for the first order scheme is

$$\max(|u|+c)\,\frac{\Delta t}{\Delta x} \le \frac{\sqrt{3}}{2},$$

this being stricter than the stability condition for MacCormack's scheme. So this is the stability condition for the hybrid scheme.

It remains to describe how the switch θ is chosen. There are many possible choices, the one selected is described in Harten [9]. Let $\Delta_{i+1/2} = \rho_{i+1} - \rho_i$. Define

$$\hat{\theta}_i = \begin{cases} \left|\dfrac{|\Delta_{i+1/2}| - |\Delta_{i-1/2}|}{|\Delta_{i+1/2}| + |\Delta_{i-1/2}|}\right|^p, & \text{for } |\Delta_{i+1/2}|+|\Delta_{i-1/2}| > \varepsilon \\ 0, & \text{otherwise.} \end{cases} \tag{37}$$

In this case $p = 1$ and $\varepsilon > 0$ is chosen as a measure of negligible variation in the density ρ. We define the switch θ by

$$\theta_{i+1/2} = \max(\hat{\theta}_i, \hat{\theta}_{i+1}).$$

Since in areas which contain a discontinuity the hybrid scheme is about first order we may apply the artificial

compression method discussed above. However, the ACM must not be used in smooth regions. For this purpose the switch is used again, i.e. equation (27b) may be replaced with

$$\underline{u}_i^{n+1} = \underline{\tilde{u}}_i^{n+1} - \frac{\Delta t}{2\Delta x}\left(\theta^n_{i+1/2}\,\underline{G}^n_{i+1/2} - \theta^n_{i-1/2}\,\underline{G}^n_{i-1/2}\right). \tag{38}$$

Antidiffusion Method of Boris and Book. In this section we shall discuss briefly the antidiffusion method developed by Boris and Book [1]. The purpose of this special technique known as "flux correction" is to achieve high resolution without oscillations.

It can be shown that a first order difference scheme can be represented by an equation of the form

$$u_t + f(u)_x = \Delta t \left[g(u,\frac{\Delta t}{\Delta x})u_x \right]_x , \tag{39}$$

where $g(u,\frac{\Delta t}{\Delta x})$ is the coefficient of the diffusion term.

The basis of the antidiffusion method is to use a stable modification of a diffusive difference scheme. Let the original scheme be represented by (39), the modification is represented by

$$u_t + f(u)_x = \Delta t \left[(g(u,\frac{\Delta t}{\Delta x}) - r(u,\frac{\Delta t}{\Delta x}))u_x \right]_x , \tag{40}$$

where r is a positive function. One can introduce the anti-diffusion term by operator splitting. The first step consists of solving

$$u_t + f(u)_x = 0, \tag{41}$$

with the original difference scheme, say $\tilde{u}_i^{n+1} = Lu_i^n$. Then in the second step let A be a difference operator approximating the diffusion equation

$$u_t + \Delta t\left[r(u,\frac{\Delta t}{\Delta x})\ u_x\right]_x = 0. \tag{42}$$

The second step is the antidiffusion step, which is unstable by itself since it approximates the backward heat equation. We define

$$u_i^{n+1} = A\tilde{u}_i^{n+1} = ALu_i^n.$$

It can be seen that if

$$g(u,\frac{\Delta t}{\Delta x}) - r(u,\frac{\Delta t}{\Delta x}) \geq 0, \tag{43}$$

then the combined scheme AL is stable. However, (43) places more of a restriction on $\frac{\Delta t}{\Delta x}$ than the stability condition for L.

We chose for L the two-step Lax-Wendroff scheme. Following Boris and Book [2], the procedure is

$$\underline{U}_{i+1/2}^{n+1/2} = \frac{1}{2}\ (\underline{U}_i^n + \underline{U}_{i+1}^n) - \frac{\Delta t}{2\Delta x}(\underline{F}_{i+1}^n - \underline{F}_i^n), \tag{44a}$$

$$\tilde{\underline{U}}_i^{n+1} = \underline{U}_i^n - \frac{\Delta t}{\Delta x}\ (\underline{F}_{i+1/2}^{n+1/2} - \underline{F}_{i-1/2}^{n+1/2}), \tag{44b}$$

$$\hat{\underline{U}}_i^{n+1} = \tilde{\underline{U}}_i^n + \eta(\underline{U}_{i+1}^n - 2\underline{U}_i^n + \underline{U}_{i-1}^n), \tag{44c}$$

$$\underline{U}_i^{n+1} = \hat{\underline{U}}_i^{n+1} - (\underline{f}_{i+1/2}^c - \underline{f}_{i-1/2}^c), \tag{44d}$$

where

$$\hat{\Delta}_{i+1/2} = \eta\,(\tilde{\underline{U}}^{n+1}_{i+1} - \tilde{\underline{U}}^{n+1}_{i}),$$

$$\Delta_{i+1/2} = \hat{\underline{U}}^{n+1}_{i+1} - \hat{\underline{U}}^{n+1}_{i},$$

$$f^{c}_{i+1/2} = \operatorname{sgn}(\hat{\Delta}_{i+1/2})\,\max\Big\{0,\ \min\Big[\operatorname{sgn}(\hat{\Delta}_{i+1/2})\Delta_{i-1/2}, |\hat{\Delta}_{i+1/2}|, \operatorname{sgn}(\hat{\Delta}_{i+1/2})\Delta_{i+3/2}\Big]\Big\}.$$

The parameter η is the diffusion/antidiffusion coefficient. The stability condition is

$$\max(|u|+c)\,\frac{\Delta t}{\Delta x} \le 1.$$

Hyman's Predictor-Corrector Method. In [12] Hyman describes a predictor-corrector type scheme. The spatial derivatives are approximated by a second order difference operator while the time derivative (or time integrator) uses the improved Euler scheme. The improved Euler scheme combines a first order explicit predictor with a second order trapazoidal rule corrector.

For stability and to insure proper entropy production an artificial viscosity term is added. The artificial viscosity term used is similar to that used by Rusanov [20].

The scheme is given by

$$\underline{u}^{n+1/2}_{i} = \underline{u}^{n}_{i} - \Delta t\,(D\underline{F}^{n}_{i} - \delta(\underline{\Phi}^{n}_{i+1/2} - \underline{\Phi}^{n}_{i-1/2})), \tag{45a}$$

$$= \underline{u}^{n}_{i} - \Delta t\,\underline{P}^{n}_{i}$$

$$\underline{u}^{n+1}_{i} = \underline{u}^{n}_{i} - \frac{\Delta t}{2}\,(D\underline{F}^{n+1/2}_{i} + \underline{P}^{n}_{i}), \tag{45b}$$

where

$$D\underline{F}_i^n = \frac{1}{12\Delta x}\left(-\underline{F}_{i+2}^n + 8\underline{F}_{i+1}^n - 8\underline{F}_{i-1}^n + \underline{F}_{i-2}^n\right),$$

$$\underline{\phi}_{i+1/2}^n = \frac{1}{4\Delta x}\left(\alpha_{i+1}^n + \alpha_i^n\right)\left(\underline{u}_{i+1}^n - \underline{u}_i^n\right),$$

$$\alpha_i^n = (u + c)_i^n,$$

and c is the local sound speed.

The stability of the scheme depends on the number of applications of the corrector (45b) and on δ. We took as the stability condition

$$\max\left(|u| + c\right)\frac{\Delta t}{\Delta x} \leq 1.$$

In order to maintain stability, the artificial viscosity must not be completely removed in the smooth regions. However, it can be reduced in these regions by using a type of switch. The one chosen was suggested by Hyman [12]. Replace $\underline{\phi}_{i+1/2}^n$ in (45a) by $\beta\,\underline{\phi}_{i+1/2}^n$ where

$$\beta = \begin{cases} \frac{1}{3}, & \text{if } \alpha_{i+1}^n > \alpha_i^n + \frac{\Delta x}{3} \\ 1, & \text{otherwise.} \end{cases}$$

This type of switch greatly reduces the smearing of the contact discontinuity as well as the shock wave. This switch is a type of artificial compression.

III. The Shock Tube Problem

Figure 2 represents the initial conditions in a shock tube. A diaphragm at x_0 separates two regions (regions 1 and 5) which have difference density and pressures. The two regions are in a constant state. The initial conditions are $p_1 > p_5$, $\rho_1 > \rho_5$, and

$u_1 = u_5 = 0$, i.e. both fluids are initially at rest. At time $t > 0$ (see Fig. 3) the diaphragm is broken. Consider the case before any wave has reached the left or right boundary. Points x_1 and x_2 represent the location of the head and tail of the rarefaction wave (moving to the left). Although the solution is continuous in this region (region 2) some of the derivatives of the fluid quantities may not be continuous. The point x_3 is the position that an element of fluid initially at x_0 has reached by time t. x_3 is called a contact discontinuity. It is seen that across a contact discontinuity the pressure and the normal component of velocity are continuous. However, the density and the tangential component of velocity are not continuous across a contact discontinuity. The point x_4 is the location of the shock wave (moving to the right). Across a shock all of the quantities (ρ, m, e, and p) will in general be discontinuous.

In the study of the above numerical methods the following test problem was considered: $\rho_1 = 1.$, $p_1 = 1.$, $u_1 = 0.$, $\rho_5 = 0.125$, $p_5 = 0.1$, and $u_5 = 0$. The ratio of specific heats γ was chosen to be 1.4. In all of the calculations $\Delta x = 0.01$. For the Rusanov scheme the value of ω was taken to be 1.0. In the scheme of Boris and Book the parameter η was taken to be 0.125. For Hyman's scheme the value of δ was taken to be 0.8. The constant in the artificial viscosity term ν was taken to be 1.0 in all but one case. Also the value of σ (see Table I) was taken to be 0.9.

In Glimm's original construction a new value of ξ was chosen for each grid point i and each time level n. The practical effect of such a choice with finite Δx is disasterous; since our initial data is not close to constant (which was an assumption made by Glimm). In fact, if ξ is chosen for each i and n, it is possible that a state will

propagate to the left and to the right and thus create a spurious state. An improvement due to Chorin [3] is to choose ξ_n only once per time step (hence the subscript n). The details of the method of selection of the random number are found in Chorin [3] and Sod [21].

Figure 4 indicates the results using the first order accurate Godunov scheme. The corners at the endpoints of the rarefaction wave are rounded. The constant state between the contact discontinuity and the shock has not been fully realized. The transition of the contact discontinuity occupies 7-8 zones while the transition of the shock occupies 5-6 zones.

Figure 5 indicates the results using the Godunov scheme with artificial compression. It should be noted that for this case the constant in the artificial viscosity term was taken to be 2.0 to insure that the solution before application of artificial compression was oscillation free. For the artificial compression cannot be applied in the presence of oscillations. The corners at the endpoints of the rarefaction wave are still rounded, since the artificial compression method is not applied in smooth regions. There is a slight undershoot at the right corner of the rarefaction. Also there are oscillations at the contact discontinuity. The transition of the contact discontinuity occupies 3-4 zones while the transition of the shock occupies only 1-2 zones.

Figure 6 shows the results of the two-step Lax Wendroff scheme. There are very slight overshoots at the contact discontinuity and more noticeable overshoots at the shock. The rarefaction wave is quite accurate. The corners at the endpoints of the rarefaction

are only slightly rounded. The transition of the contact discontinuity occupies 6-8 zones while the shock wave occupies 4-6 zones. It is observed that the plots in Figure 6 are quite similar to those in Figure 7 obtained by MacCormack's method.

Figure 7 represents the results of the second order MacCormack scheme. There are slight overshoots at the contact discontinuity and more noticeable overshoots at the shock wave. The rarefaction wave is quite accurate. The corners at the endpoints of the rarefaction are only slightly rounded. The transition of the contact discontinuity occupies 7-8 zones while the transition of the shock occupies 5-6 zones.

Figure 8 represents the first order accurate Rusanov scheme. The contact discontinuity is barely visible in the density profile. The corners at the endpoints of the rarefaction wave are extremely rounded. The constant state between the contact discontinuity and the shock wave is barely existent. The transition of the contact discontinuity occupies 14-16 zones and the transition of the shock occupies 6-8 zones. This scheme is extremely diffusive. This scheme will even diffuse entropy for zero flow fields.

Figure 9 represents the Rusanov scheme with artificial compression. The results with artificial compression are greatly improved. The corners at the endpoints of the rarefaction wave are still rounded since the artificial compression method is not applied in this area. The constant state between the contact discontinuity and the shock is much more visible. The transition of the contact discontinuity occupies 2-3 zones while that of the shock wave occupies only 1-2 zones.

Figure 10 represents the upwind difference scheme. It is observed that between the left constant state and the left endpoint of the rarefaction wave is a shock (discontinuity). This is clearly a nonphysical solution. This is a result of the method used to stabalize the scheme, by using centered differences for the pressure term in the momentum equation.

Figure 11 shows the results of the Glimm scheme. The shock wave and the contact discontinuity have been computed with infinite resolution, i.e. the number of zones over which the variation occurs is zero. Due to the randomness of the method the positions of the shock and the contact discontinuity are not exact. However, on the average their positions are exact. The corners at the endpoints of the rarefaction wave are perfectly sharp. It is observed that the rarefaction is not smooth, yet it is extremely close to the exact solution. The constant states are perfectly realized.

The Glimm scheme requires between 2 and 3 times as much time (see below) as the other finite difference schemes tested. However, the Glimm scheme requires far less spatial grid points for the same resolution. This is displayed in Table II, where 9 interior grid points are used. All details are visible.

The Glimm scheme on the average is conservative. One other check on the accuracy is to use the conservation laws (mass, momentum, and energy). For example, the total mass is

evaluated by

$$Q_\rho = \sum_i \rho(i\Delta x)\ \Delta x.$$

In Table III the values of the total mass, momentum, and energy are displayed. The mass and the energy are seen to be conserved on the average, i.e. there are fluctuations but they are contained within a small interval. The momentum is seen to increase linearly on the average (allowing for fluctuations).

Figure 12 shows the results of the antidiffusion method of Boris and Book applied to the two-step Lax-Wendroff scheme. There is a slight overshoot at the right corner of the rarefaction . The rarefaction wave is very accurately computed. The corners at the endpoints of the rarefaction are only slightly rounded. The constant state between the contact discontinuity and the shock wave is only partially realized. The transition of the contact discontinuity occupies 5-7 zones and the transition of the shock occupies 1-2 zones. The resolution is much better than the two-step Lax-Wendroff scheme alone (see Fig. 6).

Figure 13 repsents the hybrid scheme (35) and (36) of Harten and Zwas. The solution is free of oscillations. The corners at the endpoints of the rarefaction wave are only slightly rounded. The constant state between the contact discontinuity and the shock is only partly realized. The trans-

ition of the contact discontinuity occupies 8-9 zones and the transition of the shock occupies 5-6 zones.

Figure 14 represents the hybrid scheme of Harten and Zwas with the use of artifical compression. Since the artifical compression is not applied in smooth regions the rarefaction is the same as in Fig. 13. The transition of the contact discontinuity occupies 3-4 zones and the transition of the shock wave occupies 2-3 zones.

Figure 15 represents the results of Hyman's predictor-corrector scheme, where the corrector has been applied once. The solution is oscillation free. The corners at the endpoints of the rarefaction are almost perfectly sharp. The constant states between the rarefaction and the contact discontinuity and between the contact discontinuity are extremely well defined. The transition of the contact discontinuity occupies 6-8 zones while the transition of the shock occupies 3-4 zones.

The timing results for all of the methods are listed in Table IV. The times are for 100 spatial grid points. The only substantial difference in timing is between Glimm's scheme and the other finite difference schemes. For Glimm's scheme requires between 2 and 3 times as much time. However, Glimm's scheme can give the same resolution with far less points (as seen in Table II). From the point of view of the least number of grid points per desired resolution, the Glimm scheme can be seen to be much faster.

IV. Conclusions

Of all the finite difference schemes tested, without the use of corrective procedures, Godunov's and Hyman's methods

produced the best results.

It is obvious from the figures that the Glimm scheme gives the best resolution of the shocks and contact discontinuities.

Glimm's scheme is at best first order accurate (see Chorin [3]) so that boundary conditions are easily handled.

It is possible that the rarefaction wave obtained by Glimm's method can be smoothed out by a type of averaging. This is presently being considered.

The hybrid method of Harten and Zwas combines first and high order schemes in such a way as to extract the best features of both. The high order scheme produces better approximations to the smooth parts of the flow.

The corrective procedures of Boris and Book and Harten improve the resolution of a given scheme. The artifical compression method being restricted to first order schemes except when used in conjunction with the hybird type schemes produces far better results than the antidiffusion method of Boris and Book. Both methods are easily added to existing programs (as a subroutine). The antidiffusion method requires slightly more storage than the artificial compression method since the former must retain two time levels of information for the computation of intermediate results (equation (44c)).

A major disadvantage of the antidiffusion method of Boris and Book, the hybrid scheme of Harten and Zwas, and the artificial compression method of Harten is that there are a number of parameters to be chosen, which depend on the given problem. In the antidiffusion method the coefficient of diffusion/antidiffusion must be chosen. The value of this parameter can greatly affect the results. In the hybrid

scheme a tolerance must be chosen for the automatic switch which is taken to be a measure of negligible variation in entropy or density for example. This tolerance depends on the given problem. In the artificial compression method a test must be included to locate the rarefaction (and other smooth regions). Many of the standard tests fail to work well enough for the use of artificial compression.

With the method described for solving the Riemann problem in the Glimm scheme, it can only be used for the equations of gas dynamics in rectangular coordinates. It is possible to generalize Glimm's method to other coordinate systems and different equations. See Harten and Sod [10].

The applicability of Glimm's method to other geometries has only just started to be explored. One successful application is to the equations of gas dynamics for a cylindrically or spherically symmetric flow. See Sod [22].

Acknowledgements

The author would like to thank Professor Alexandre Chorin, Mr. Phillip Colella, Dr. Amiram Harten, and Dr. James M. Hyman for a number of helpful discussions and comments. The author would also like to thank Josette Bordiga for her encouragement without which this would not be possible.

This work was also supported in part by the National Science Foundation, Grant MCS76-07039.

Appendix: Implementation of Glimm's Method

In this appendix we discuss the equations required for the computer implementation of Glimm's method.

As in Fig. 1, the fluid initially at $x \leq 0$ is separated from the fluid initially at $x > 0$ by a slip line $\frac{dx}{dt} = u_*$. There are a total of 10 cases to consider.

I. The sample point $\xi_n \Delta x$ lies to the left of the slip line ($\xi_n \Delta x < u_* \Delta t/2$).

(a) If the left wave is a shock wave ($p_* > p_\ell$) and (1) if $\xi_n \Delta x$ lies to the left of the shockline $\frac{dx}{dt} = U_\ell$, we have $\rho = \rho_\ell$, $u = u_\ell$, and $p = p_\ell$, (2) if $\xi_n \Delta x$ lies to the right of the shockline $\frac{dx}{dt} = U_\ell$, we have $\rho = \rho_*$, $u = u_*$, $p = p_*$, where ρ_* can be obtained from (13)

$$\rho_* = \frac{M_\ell}{U_\ell - u_*} . \tag{46}$$

(b) If the left wave is a rarefaction wave ($p_* \leq p_\ell$). Define the sound speed to be $c = \sqrt{\frac{\gamma p}{\rho}}$. The rarefaction wave is bounded on the left by the line defined by $\frac{dx}{dt} = u_\ell - c_\ell$, where $c_\ell = \sqrt{\frac{\gamma p_\ell}{\rho_\ell}}$, and on the right by the line defined by $\frac{dx}{dt} = u_* - c_*$, where $c_* = \sqrt{\frac{\gamma p_*}{\rho_*}}$. The flow is adiabatic in smooth regions, so in this region A(S) in (4b) is a constant, denoted by A, and we obtain the isentropic law $p = A\rho^\gamma$. ρ_* is obtained by using the isentropic law

$$p_\ell \rho_\ell^{-\gamma} = p_* \rho_*^{-\gamma} = A . \tag{47}$$

Then we obtain from (46)

$$\rho_* = \left(\frac{p_*}{A}\right)^{1/\gamma} . \tag{48}$$

(1) If $\xi_n \Delta x$ lies to the left of the rarefaction wave, then $\rho = \rho_\ell$, $u = u_\ell$, and $p = p_\ell$.

(2) If $\xi_n \Delta x$ lies inside the left rarefaction wave, we equate the slope of the characteristic $\frac{dx}{dt} = u - c$ to the slope of the line through the origin and $(\xi_n \Delta x, \Delta t/2)$, obtaining

$$u - c = \frac{2\xi_n \Delta x}{\Delta t} . \tag{49}$$

With the constancy of the Riemann invariant

$$2c(\gamma-1)^{-1} + u = 2c_\ell(\gamma-1)^{-1} + u_\ell , \tag{50}$$

the isentropic law, and the definition of c, we can obtain ρ, u, and p. Using the isentropic law we obtain

$$p = p_\ell \rho_\ell^{-\gamma} \rho^\gamma = A\rho^\gamma . \tag{51}$$

Using equation (50) we obtain, by solving for c

$$c = c_\ell + \frac{\gamma-1}{2}(u_\ell - u) . \tag{52}$$

By substitution of (52) into (49) and solving for u we obtain

$$u = \frac{2}{\gamma+1}\left(\frac{2\xi_n \Delta x}{\Delta t} + c_\ell + \frac{(\gamma-1)}{2} u_\ell\right) . \tag{53}$$

By substitution of (53) into (52) c is obtained; by substitution of (52) into the definition of c and solving for ρ we obtain

$$\rho = \left(\frac{c^2}{\gamma A}\right)^{1/\gamma-1} . \qquad (53)$$

(3) If $\xi_n\Delta x$ lies to the right of the left rarefaction wave we obtain $\rho = \rho_*$, $u = u_*$, and $p = p_*$.

II. The sample point $\xi_n\Delta x$ lies to the right of the slip line ($\xi_n\Delta x \geq u_*\Delta t/2$).

(a) If the right wave is a shock wave ($p_* > p_r$) and (i) if $\xi_n\Delta x$ lies to the left of the shockline defined by $\frac{dx}{dt} = U_r$, we have $\rho = \rho_*$, $u = u_*$, and $p = p_*$, where ρ_* is obtained from (15)

$$\rho_* = \frac{-M_r}{u_* - U_r} . \qquad (54)$$

(2) If $\xi_n\Delta x$ lies to the right of the shockline defined by $\frac{dx}{dt} = U_r$, we have $\rho = \rho_r$, $u = u_r$, and $p = p_r$.

(b) If the right wave is a rarefaction wave ($p_* \leq p_r$). The rarefaction wave is bounded on the left by the line defined by $\frac{dx}{dt} = u_* + c_*$, where $c_* = \sqrt{\frac{\gamma\rho_*}{\rho_*}}$ and ρ_* can be obtained from the isentropic law

$$p_r\rho_r^{-\gamma} = p_*\rho_*^{-\gamma} = A . \qquad (55)$$

Then we obtain from (55)

$$\rho_* = \left(\frac{p_*}{A}\right)^{1/\gamma} ; \qquad (56)$$

and on the right by the line defined by $\frac{dx}{dt} = u_r + c_r$, $c_r = \sqrt{\frac{\gamma p_r}{\rho_r}}$.

(1) If $\xi_n\Delta x$ lies to the left of the rarefaction wave, then $\rho = \rho_*$, $u = u_*$, and $p = p_*$.

(2) If $\xi_n \Delta x$ lies inside the right rarefaction wave, we equate the slope of the characteristic $\frac{dx}{dt} = u + c$ to the slope of the line through the origin and $(\xi_n \Delta x, \Delta t/2)$, obtaining

$$u + c = \frac{2\xi_n \Delta x}{\Delta t} \quad . \tag{57}$$

With the constancy of the Riemann invariant

$$2c(\gamma-1)^{-1} - u = 2c_r(\gamma-1)^{-1} - u_r \tag{58}$$

the isentropic law, and the definition of c, we can obtain ρ, u, and p. Using the isentropic law we obtain

$$p = p_r \rho_r^{-\gamma} \rho^{\gamma} = A\rho^{\gamma} \quad . \tag{59}$$

Using equation (58) we obtain, by solving for c

$$c = c_r + \frac{\gamma-1}{2}(u - u_r) \quad . \tag{60}$$

Substitution of (60) into (57) and solving for u we obtain

$$u = \frac{2}{\gamma+1}\left(\frac{2\xi_n \Delta x}{\Delta t} - c_r + \frac{\gamma-1}{2} u_r\right) \quad . \tag{61}$$

By substitution of (61) into (60) c is obtained; by substitution of (59) into the definition of c and solving for ρ we obtain

$$\rho = \left(\frac{c^2}{\gamma A}\right)^{1/\gamma-1} \quad . \tag{62}$$

(3) If $\xi_n \Delta x$ lies to the right of the right rarefaction wave we obtain $\rho = \rho_r$, $u = u_r$, and $p = p_r$.

Equations (46) - (62) are the key to the programming of Glimm's method. For a summary see the flow chart, Fig. 16 .

Table I

ORIGINATOR	ORDER	SCHEME	STABILITY*
Godunov	1	$\underline{U}_{i+1/2}^{n+1/2} = \frac{1}{2}(\underline{U}_{i+1}^{n} + \underline{U}_{i}^{n}) - \frac{\Delta t}{\Delta x}(\underline{F}_{i+1}^{n} - \underline{F}_{i}^{n})$ $\underline{U}_{i}^{n+1} = \underline{U}_{i}^{n} - \frac{\Delta t}{\Delta x}(\underline{F}_{i+1/2}^{n+1/2} - \underline{F}_{i-1/2}^{n+1/2})$	$\sigma \leq 1$
Lax-Wendroff (two-step)	2	$\underline{U}_{i+1/2}^{n+1/2} = \frac{1}{2}(\underline{U}_{i+1}^{n} + \underline{U}_{i}^{n}) - \frac{\Delta t}{2\Delta x}(\underline{F}_{i+1}^{n} - \underline{F}_{i}^{n})$ $\underline{U}_{i}^{n+1} = \underline{U}_{i}^{n} - \frac{\Delta t}{\Delta x}(\underline{F}_{i+1/2}^{n+1/2} - \underline{F}_{i-1/2}^{n+1/2})$	$\sigma \leq 1$
MacCormack	2	$\underline{U}_{i}^{\overline{n+1}} = \underline{U}_{i}^{n} - \frac{\Delta t}{\Delta x}(\underline{F}_{i+1}^{n} - \underline{F}_{i}^{n})$ $\underline{U}_{i}^{n+1} = \frac{1}{2}(\underline{U}_{i}^{n} + \underline{U}_{i}^{\overline{n+1}}) - \frac{\Delta t}{2\Delta x}(\underline{F}_{i}^{\overline{n+1}} - \underline{F}_{i-1}^{\overline{n+1}})$	$\sigma \leq 1$
Rusanov	1	$\underline{U}_{i}^{n+1} = \underline{U}_{i}^{n} - \frac{\Delta t}{2\Delta x}(\underline{F}_{i+1}^{n} - \underline{F}_{i-1}^{n}) +$ $\frac{1}{4}((\alpha_{i+1}^{n} + \alpha_{i}^{n})(\underline{U}_{i+1}^{n} - \underline{U}_{i}^{n}) -$ $(\alpha_{i}^{n} - \alpha_{i-1}^{n})(\underline{U}_{i}^{n} - \underline{U}_{i-1}^{n}))$, $\alpha_{i}^{n} = \omega\frac{\Delta t}{\Delta x}(u+c)_{i}^{n}$	$\sigma \leq 1$ $\sigma \leq \omega \leq \frac{1}{\sigma}$

*$\sigma = \max(|u| + c)\frac{\Delta t}{\Delta x}$, where c denotes the local sound speed.

Table I continued

Upwind	1	$\underline{U}_i^{n+1} = \underline{U}_i^n - \text{sgn}(u_i^n)\,\frac{\Delta t}{\Delta x}\,(\underline{U}_i^n - \underline{U}_{i+s(u)}^n) - \frac{\Delta t}{2\Delta x}\,(\underline{S}_{i+1}^n - \underline{S}_{i-1}^n)$, where $\underline{S} = (0,p,0)^T$ and $s(u) = \begin{cases} -1 \text{ if } u_i^n > 0 \\ 1 \text{ if } u_i^n < 0 \end{cases}$	$\sigma \leq 1$

Table II

x	ρ	u	p	e	Γ_+ *
0.1	1.000	0.000	1.000	2.500	2.958
0.2	1.000	0.000	1.000	2.500	2.958
0.3	0.869	0.164	0.822	2.363	2.958
0.4	0.426	0.927	0.303	1.778	2.958
0.5	0.426	0.927	0.303	1.778	2.958
0.6	0.426	0.927	0.303	1.778	2.958
0.7	0.426	0.927	0.303	1.778	2.958
0.8	0.266	0.927	0.303	2.853	3.624
0.9	0.125	0.000	0.100	2.000	2.646

* Γ_+ is the Riemann invariant $\frac{c}{\gamma-1} + \frac{u}{2}$, where c is the local sound speed.

Table III

$t/\Delta t$	Q_ρ	Q_m	Q_e
1	0.547	0.018	2.213
2	0.550	0.019	2.217
3	0.554	0.032	2.218
4	0.550	0.039	2.219
5	0.552	0.047	2.223
6	0.550	0.059	2.222
7	0.549	0.070	2.221
8	0.550	0.079	2.224
9	0.545	0.090	2.232
10	0.546	0.097	2.247
11	0.548	0.110	2.258
12	0.545	0.119	2.267
13	0.549	0.122	2.266
14	0.552	0.136	2.266
15	0.549	0.143	2.269
16	0.553	0.149	2.275
17	0.550	0.158	2.266
18	0.546	0.164	2.267
19	0.550	0.178	2.267
20	0.543	0.190	2.272

Table IV*

SCHEMES	WITHOUT ACM	WITH ACM
Godunov	0.226	0.247
Lax-Wendroff	0.226	-
MacCormack	0.224	-
Rusanov	0.224	0.240
Upwind	0.225	-
Glimm	0.364	-
Antidiffusion	0.242	-
Hybrid	0.258	0.269
Hyman	0.276	-

* Times include computation of exact solution, calls to printing and plotting routines, which were the same for all cases.

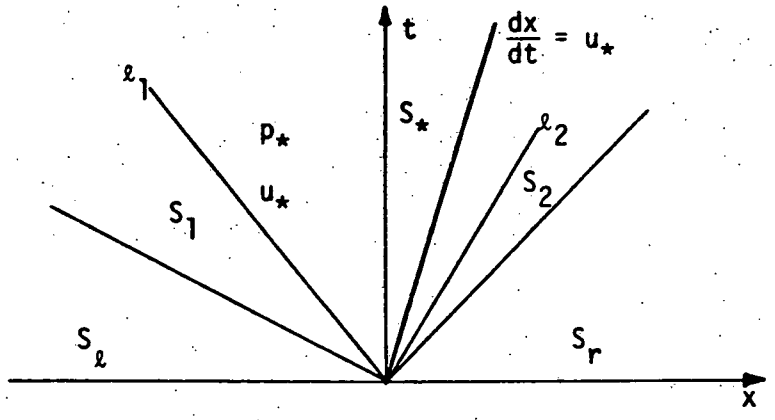

Figure 1

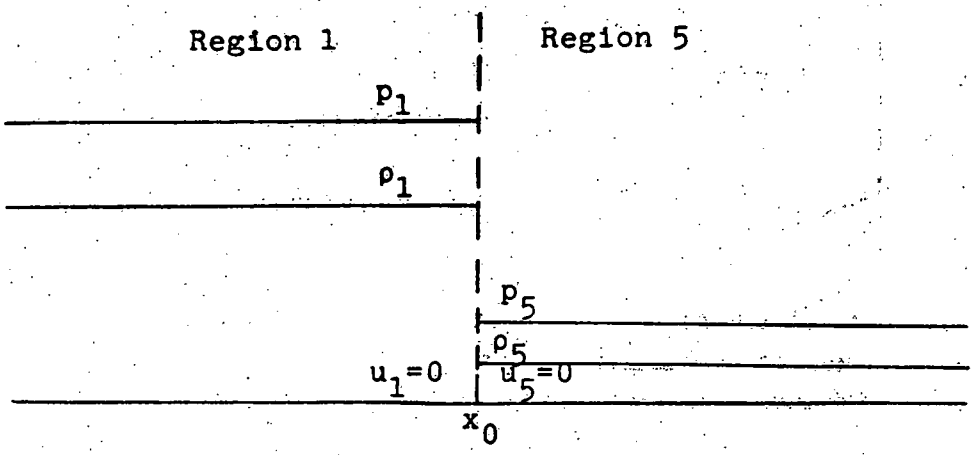

Figure 2

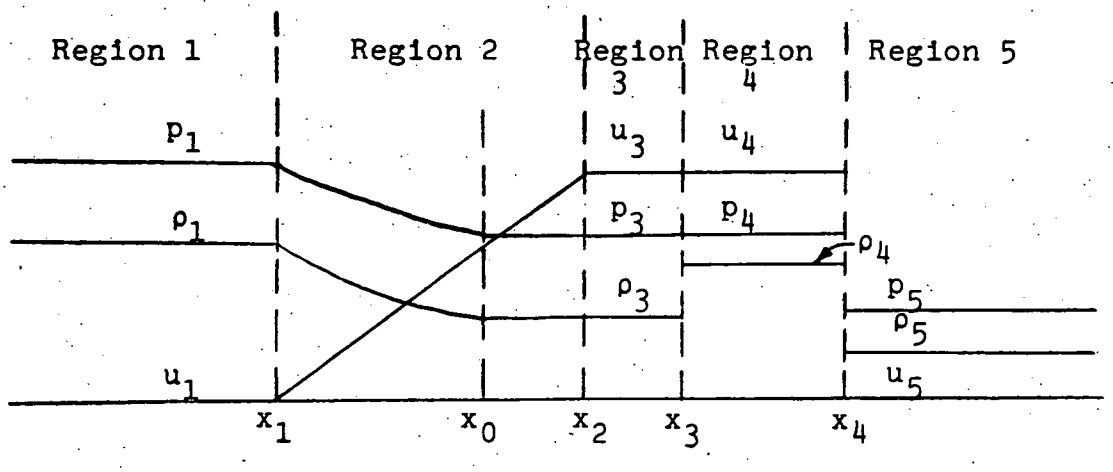
Region 1
Region 2
Region 3
Region 4
Region 5
p_1
ρ_1
u_1
u_3
u_4
p_3
p_4
ρ_4
ρ_3
p_5
ρ_5
u_5
x_1
x_0
x_2
x_3
x_4

Figure 3

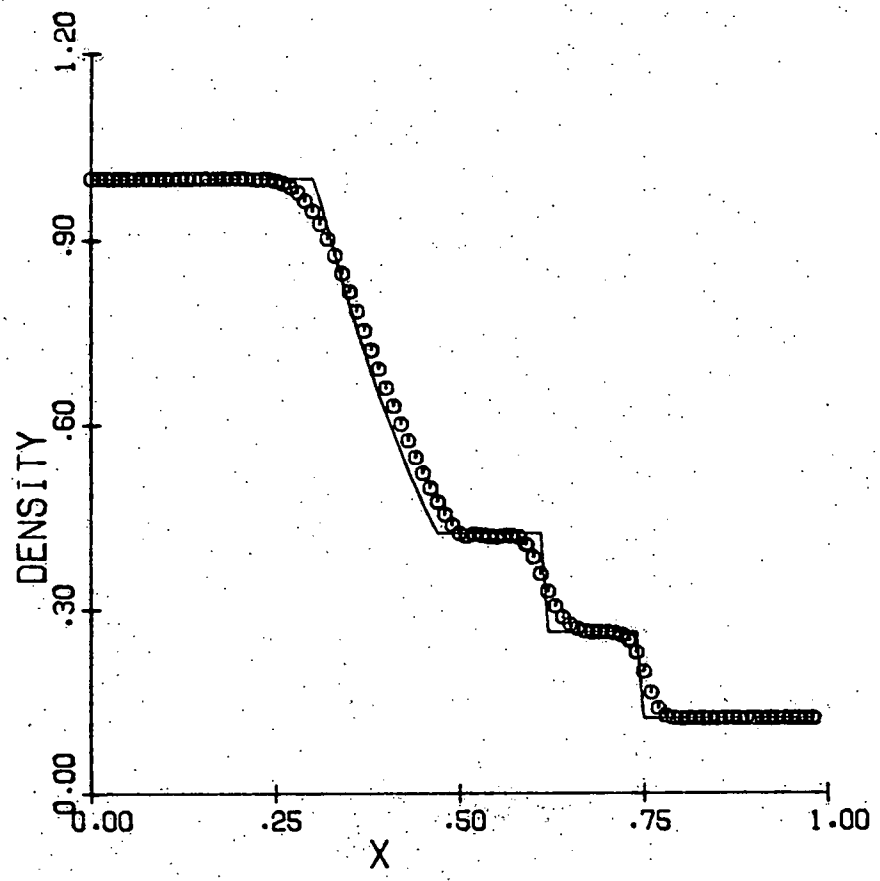
DENSITY
1.20
.90
.60
.30
0.00
0.00
.25
.50
.75
1.00
X

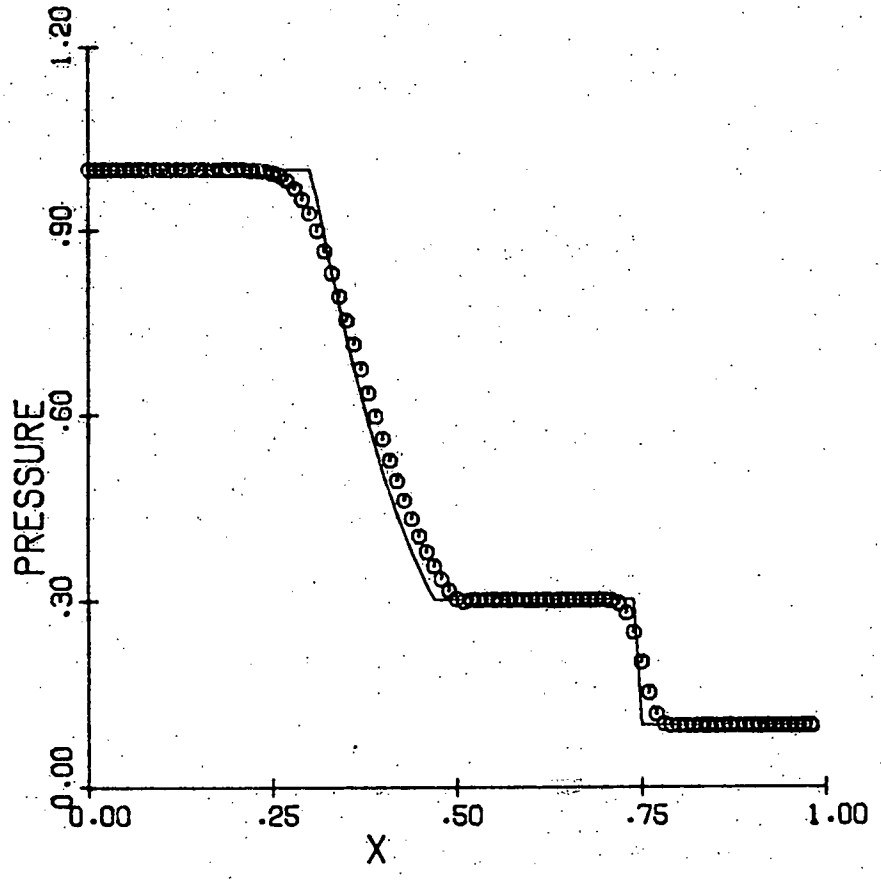
PRESSURE
1.20
.90
.60
.30
0.00
0.00
.25
.50
.75
1.00
X

Figure 4

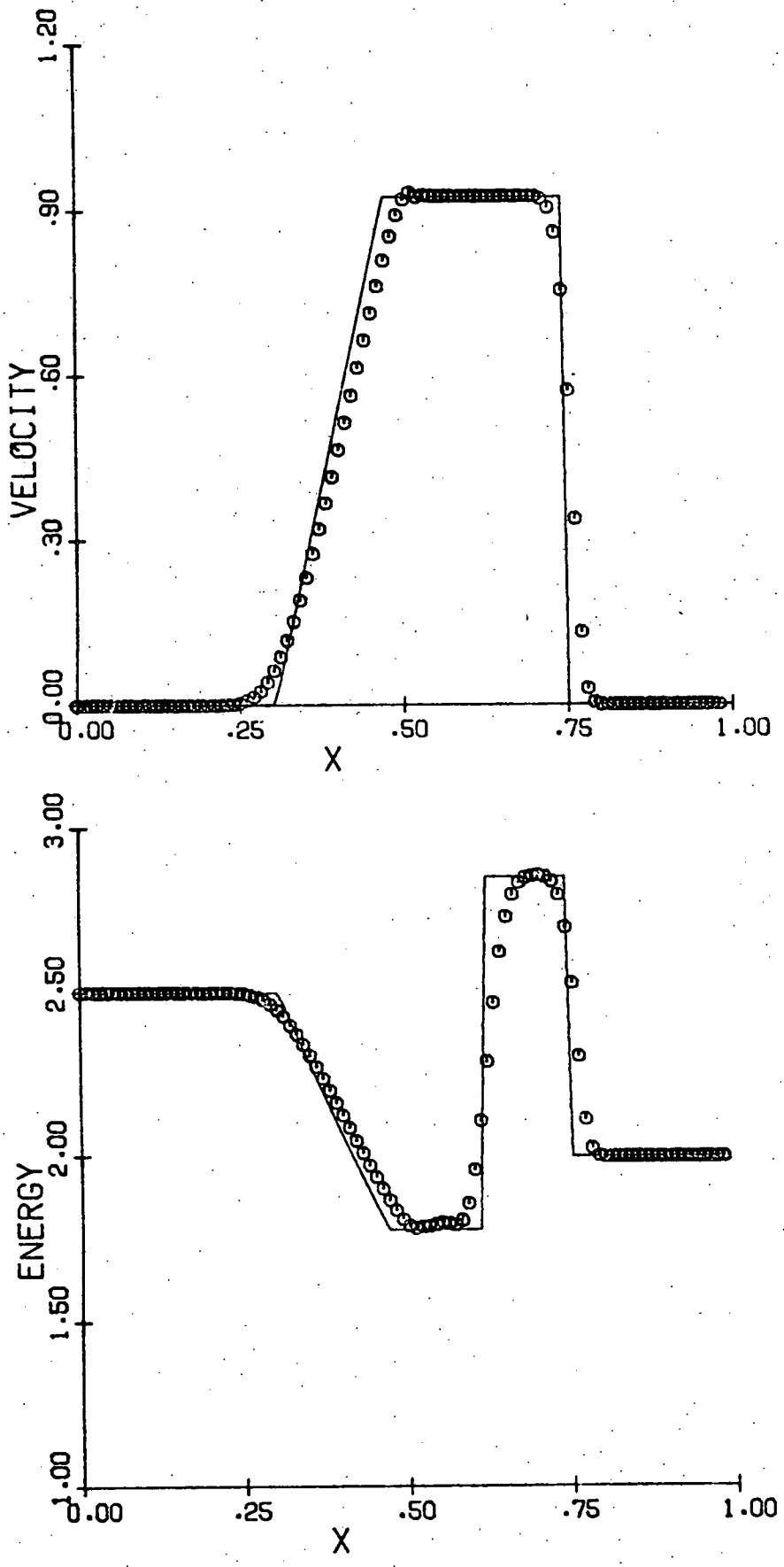

Figure 4 continued

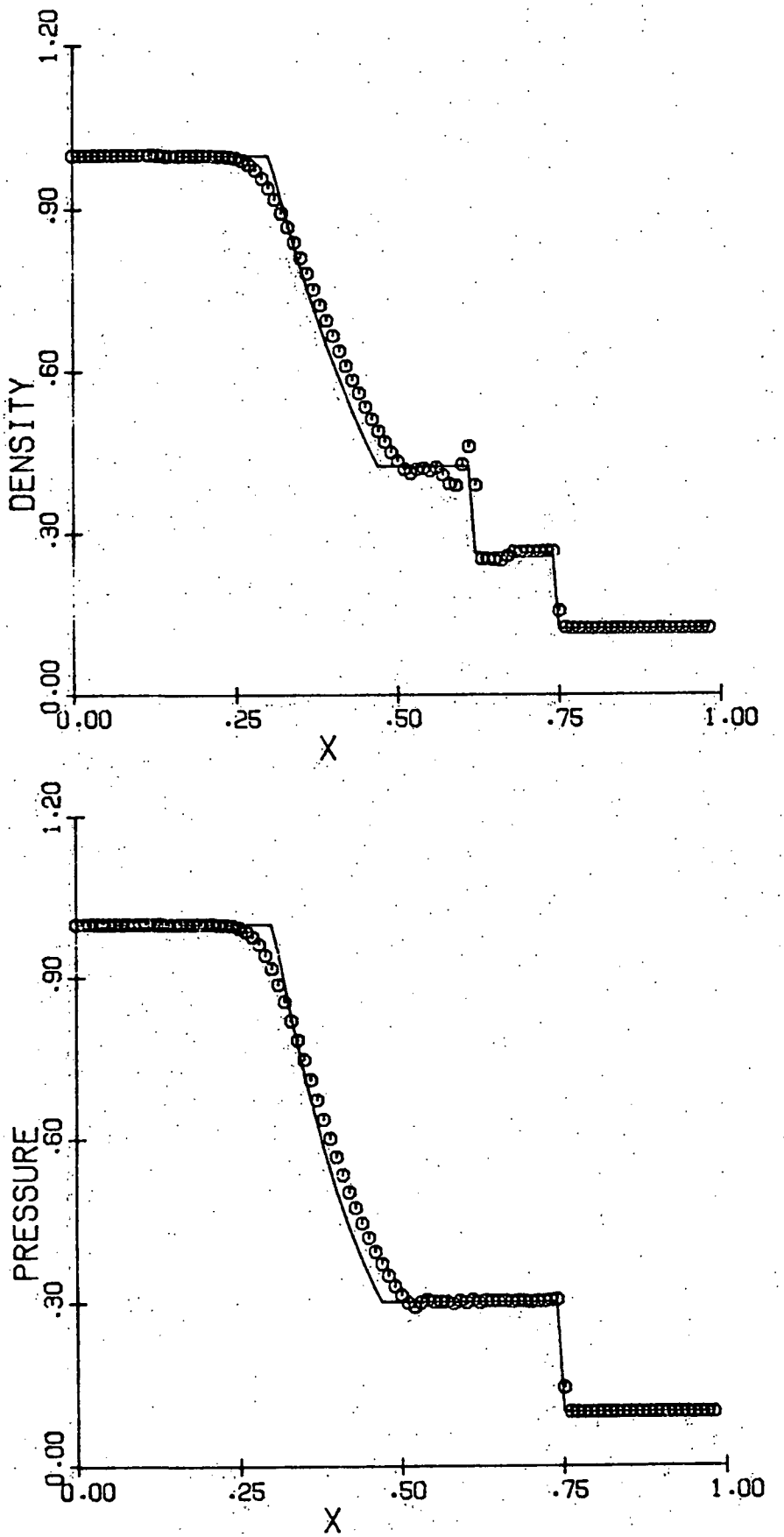
DENSITY
1.20
.90
.60
.30
0.00
0.00
.25
.50
.75
1.00
X
PRESSURE
1.20
.90
.60
.30
0.00
0.00
.25
.50
.75
1.00
X

Figure 5

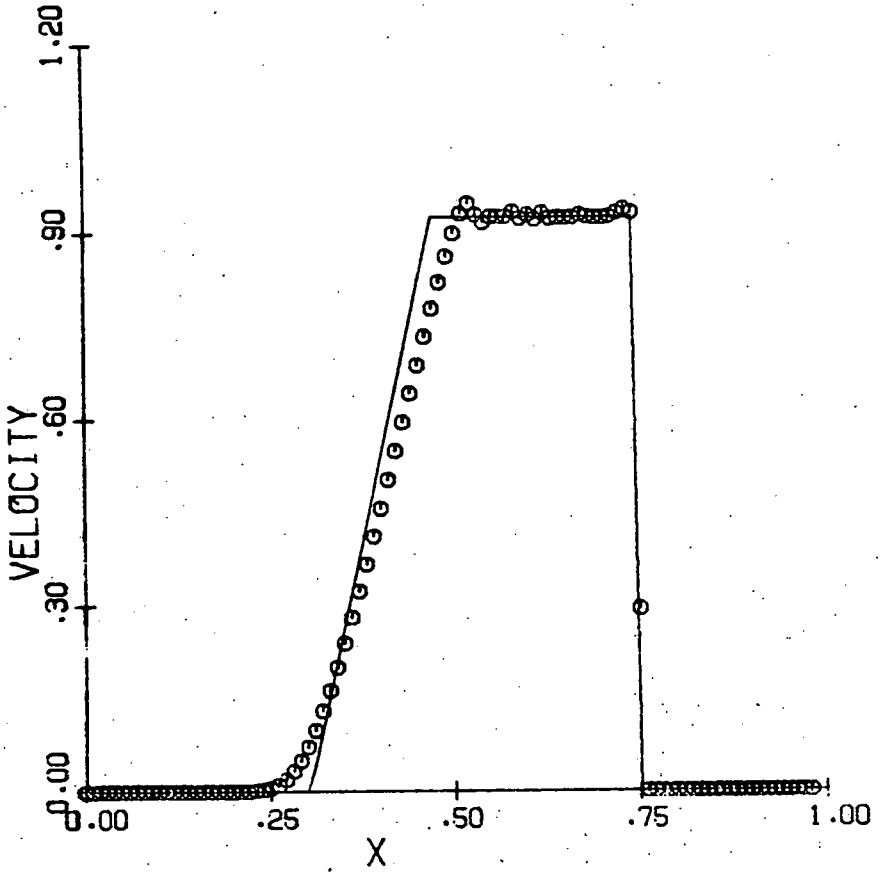

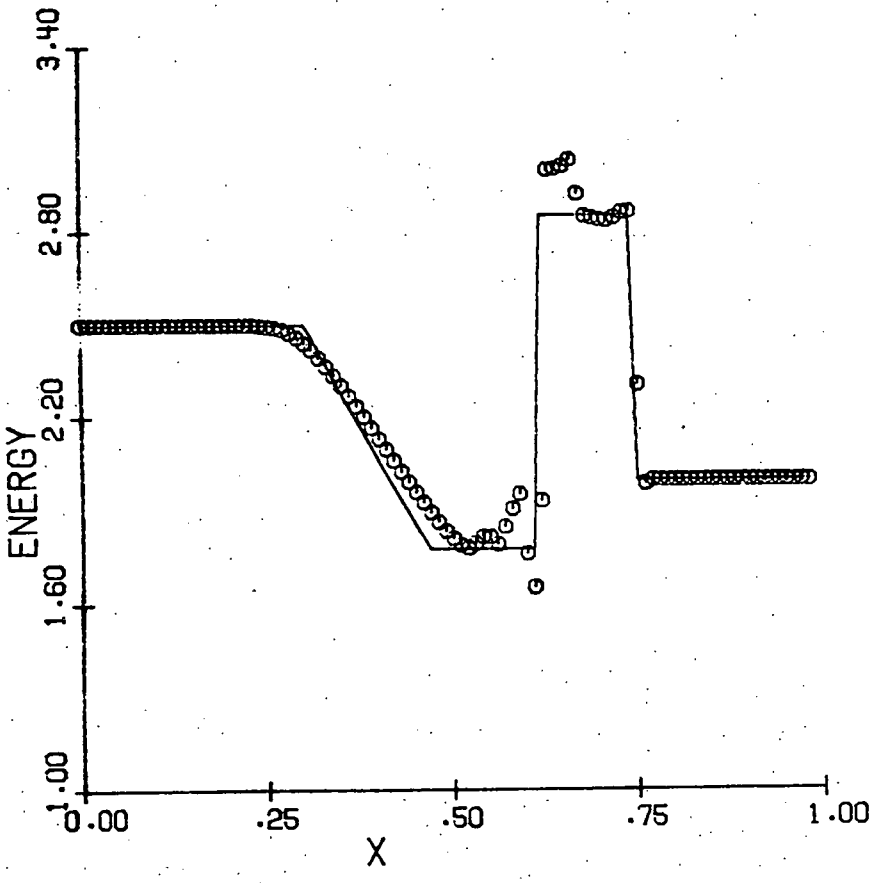

Figure 5 continued

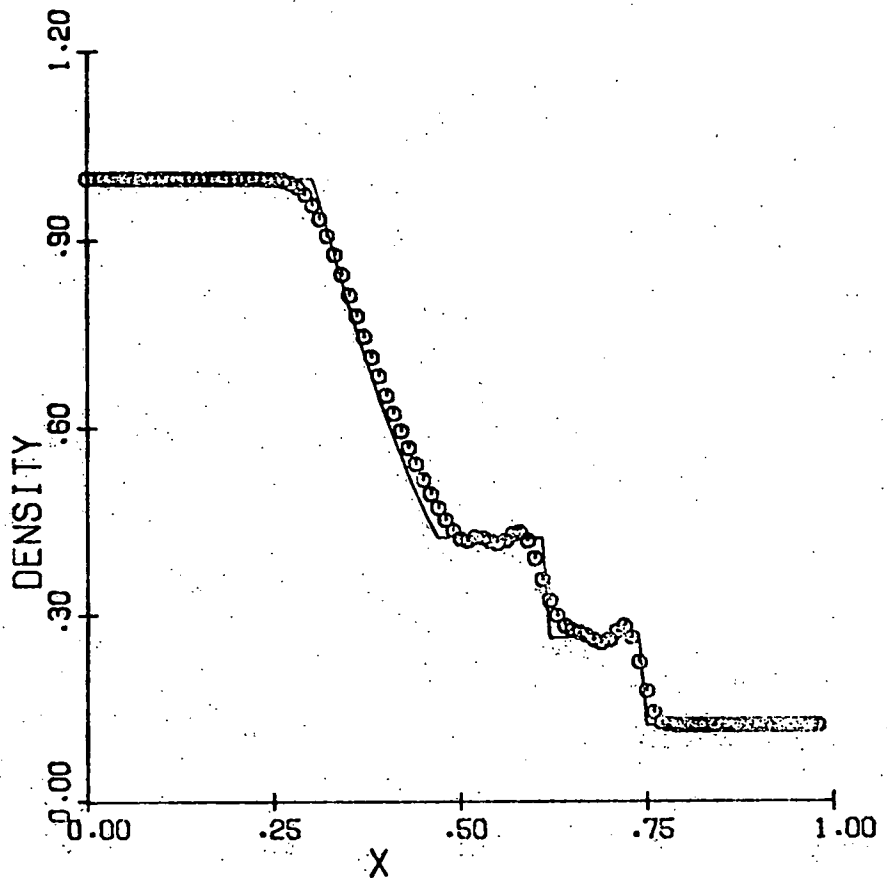
DENSITY
1.20
.90
.60
.30
0.00
0.00
.25
.50
.75
1.00
X

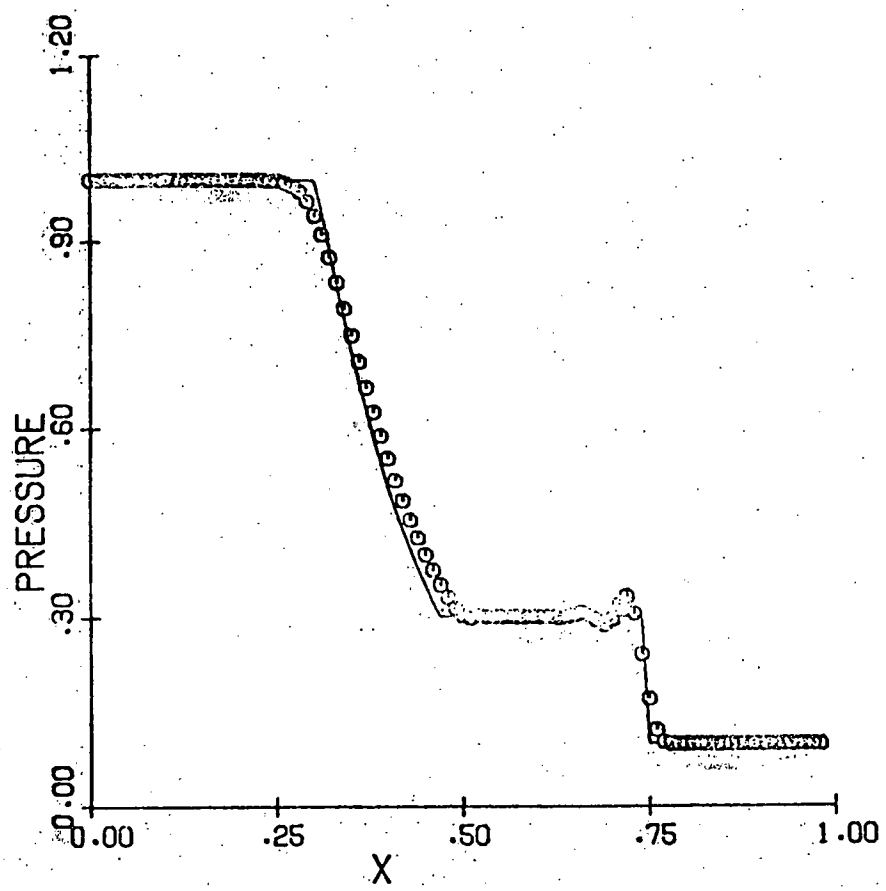
PRESSURE
1.20
.90
.60
.30
0.00
0.00
.25
.50
.75
1.00
X

Figure 6

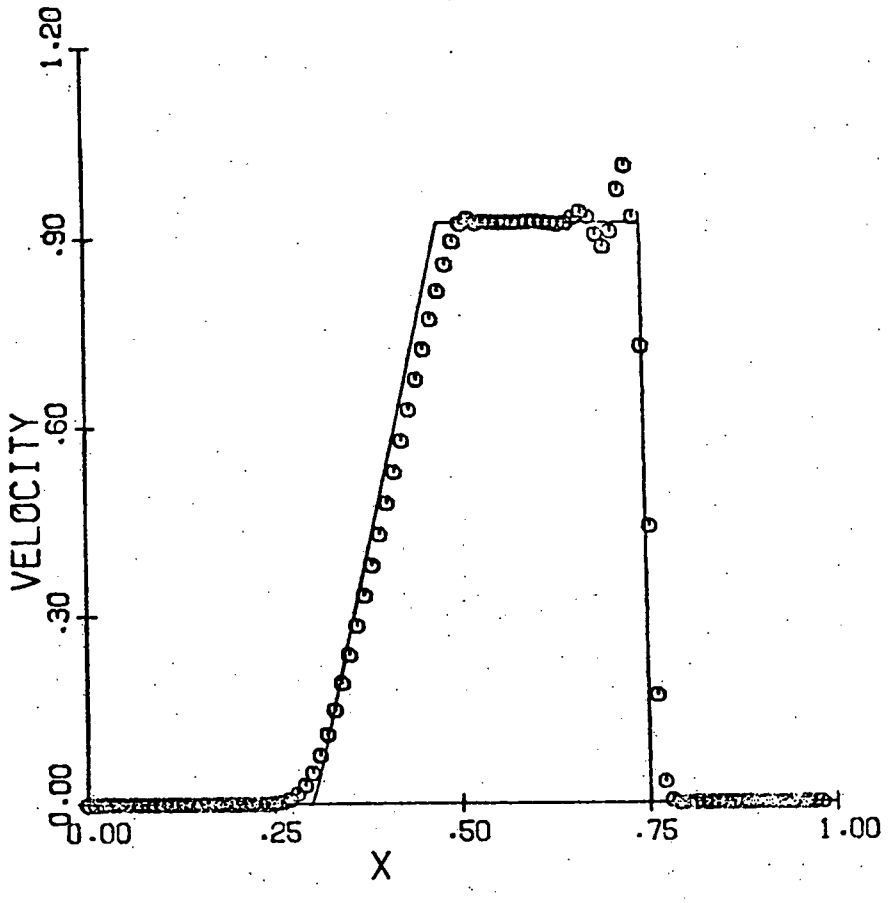

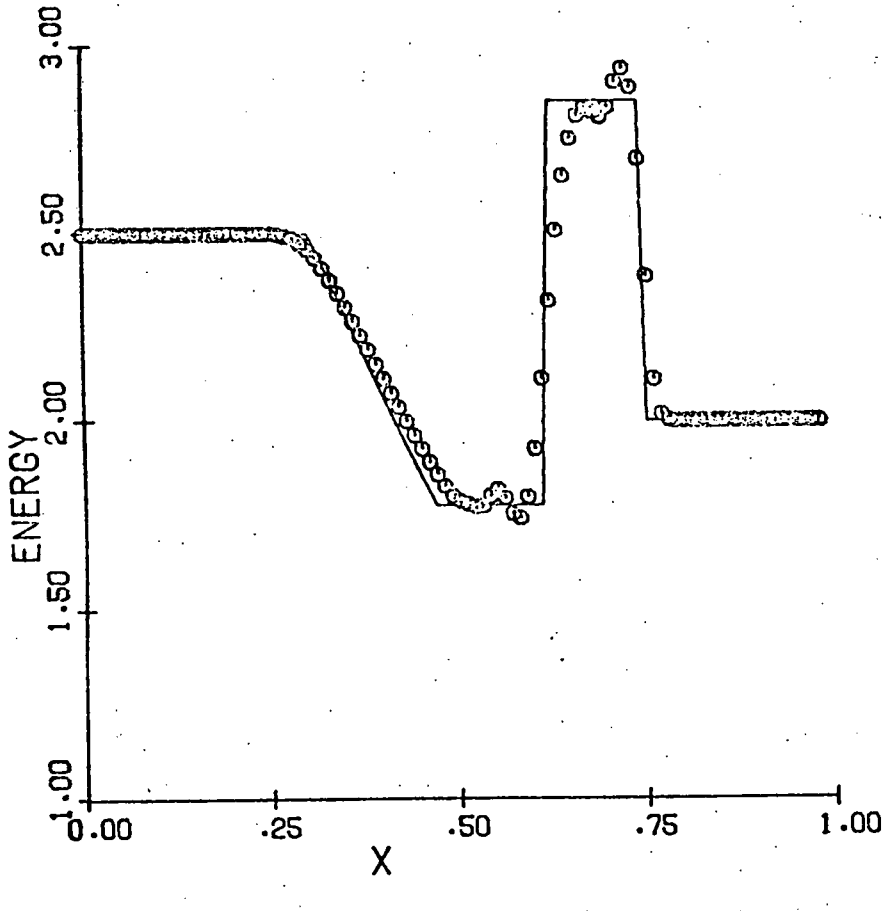

Figure 6 continued

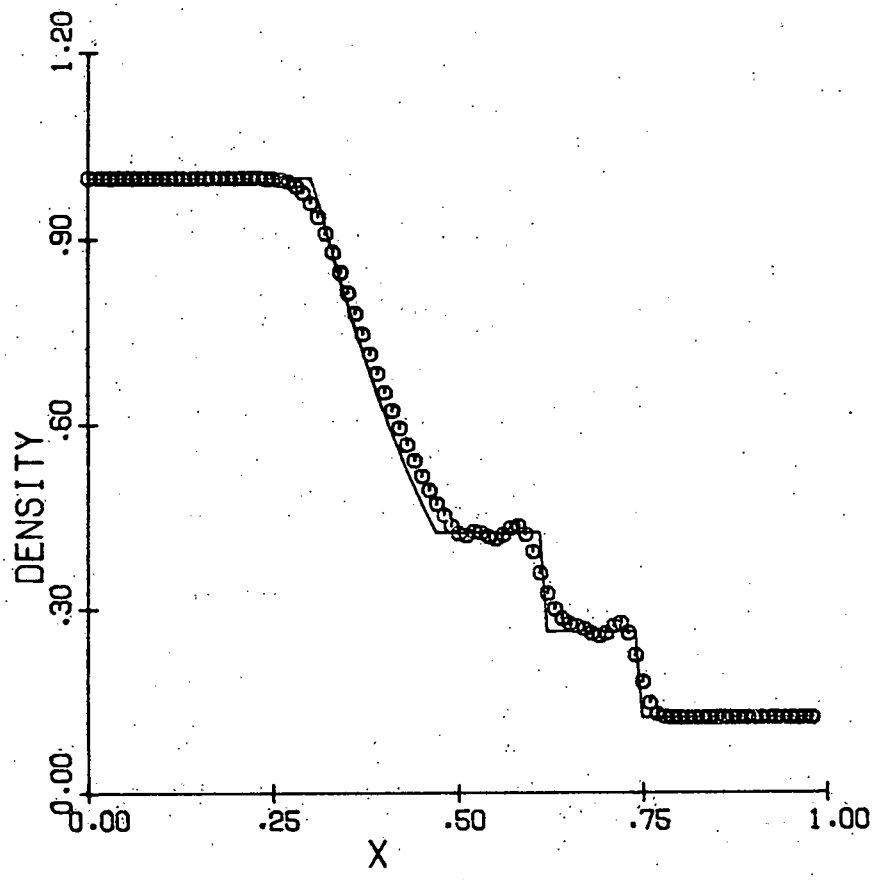
DENSITY
1.20
.90
.60
.30
0.00
0.00
.25
.50
.75
1.00
X

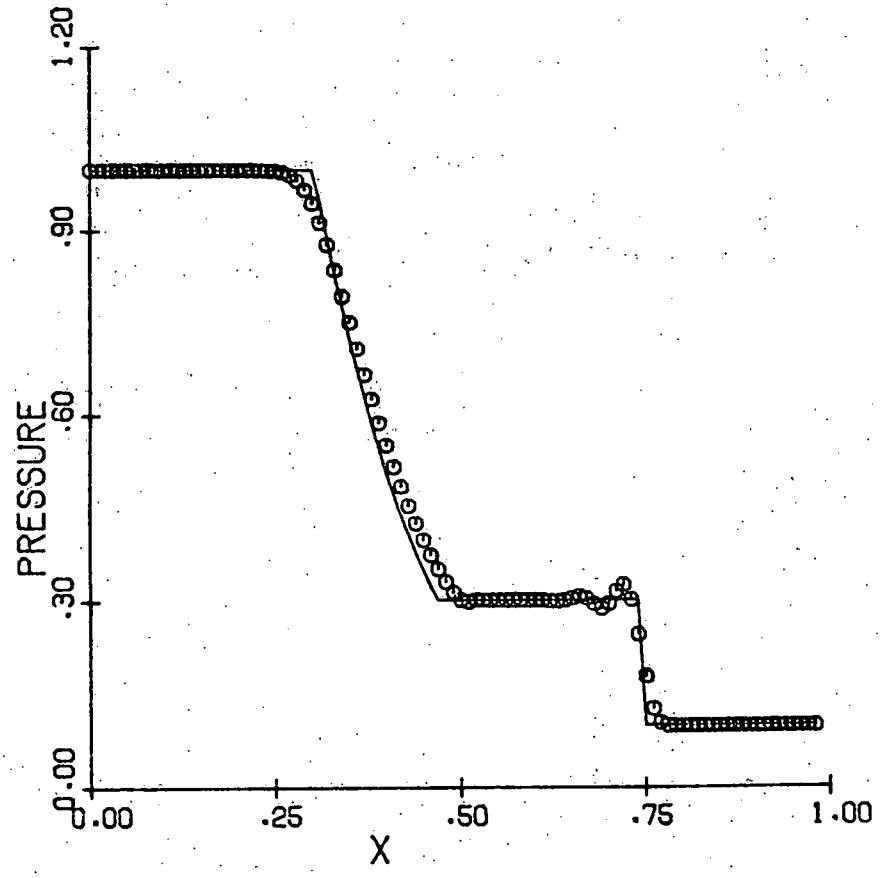
PRESSURE
1.20
.90
.60
.30
0.00
0.00
.25
.50
.75
1.00
X

Figure 7

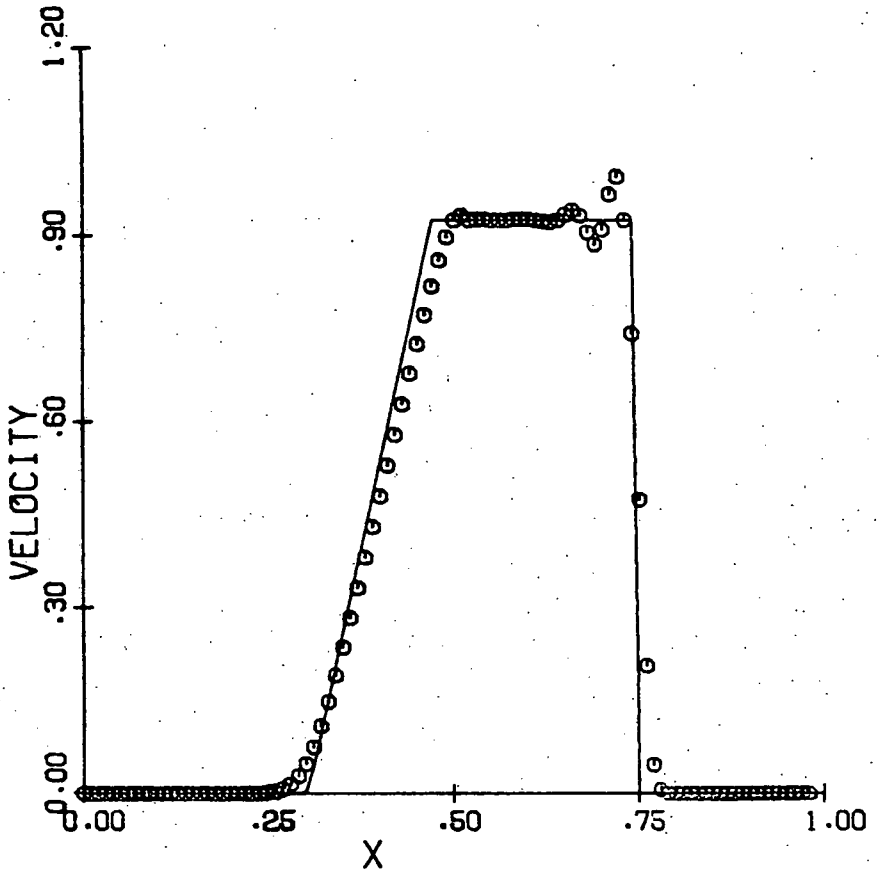

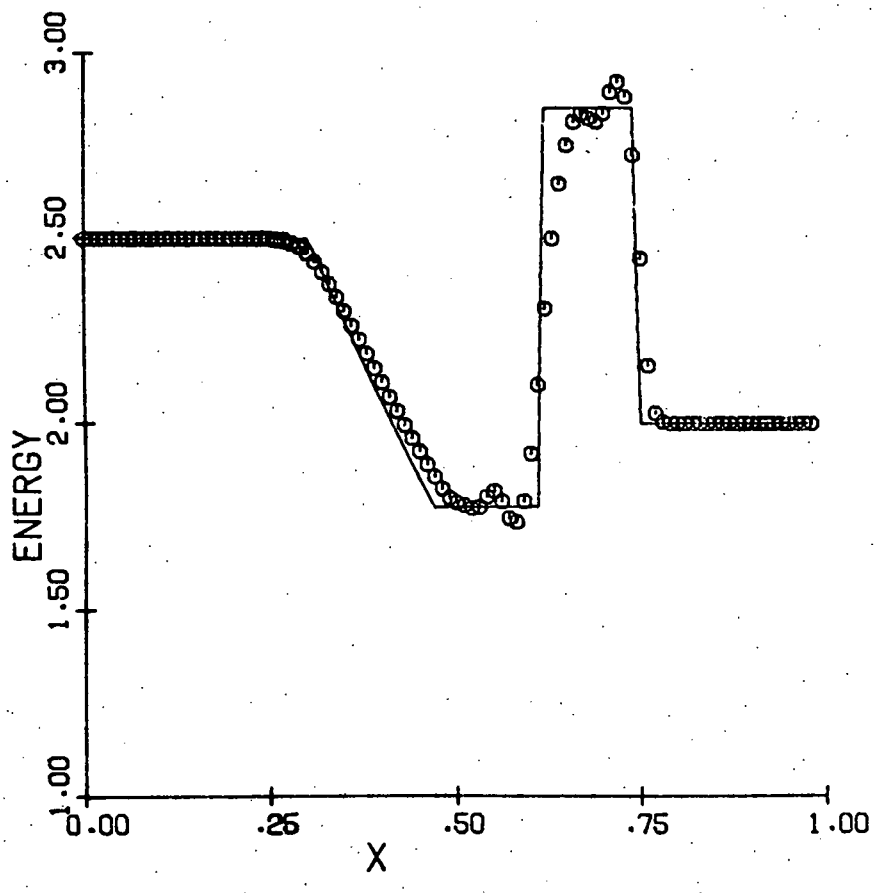

Figure 7 continued

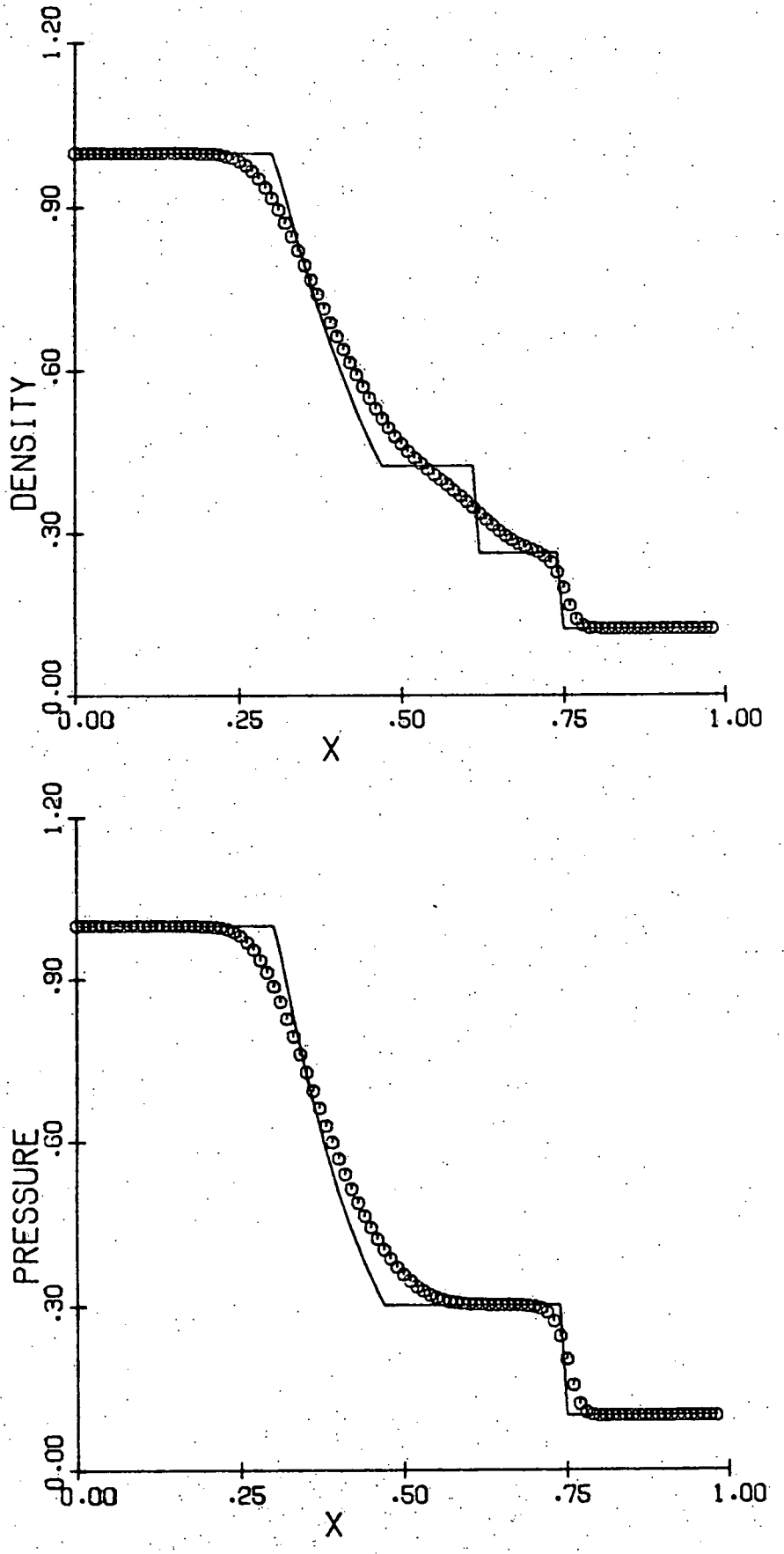
DENSITY
1.20
.90
.60
.30
0.00
0.00
.25
.50
.75
1.00
X
PRESSURE
1.20
.90
.60
.30
0.00
0.00
.25
.50
.75
1.00
X

Figure 8

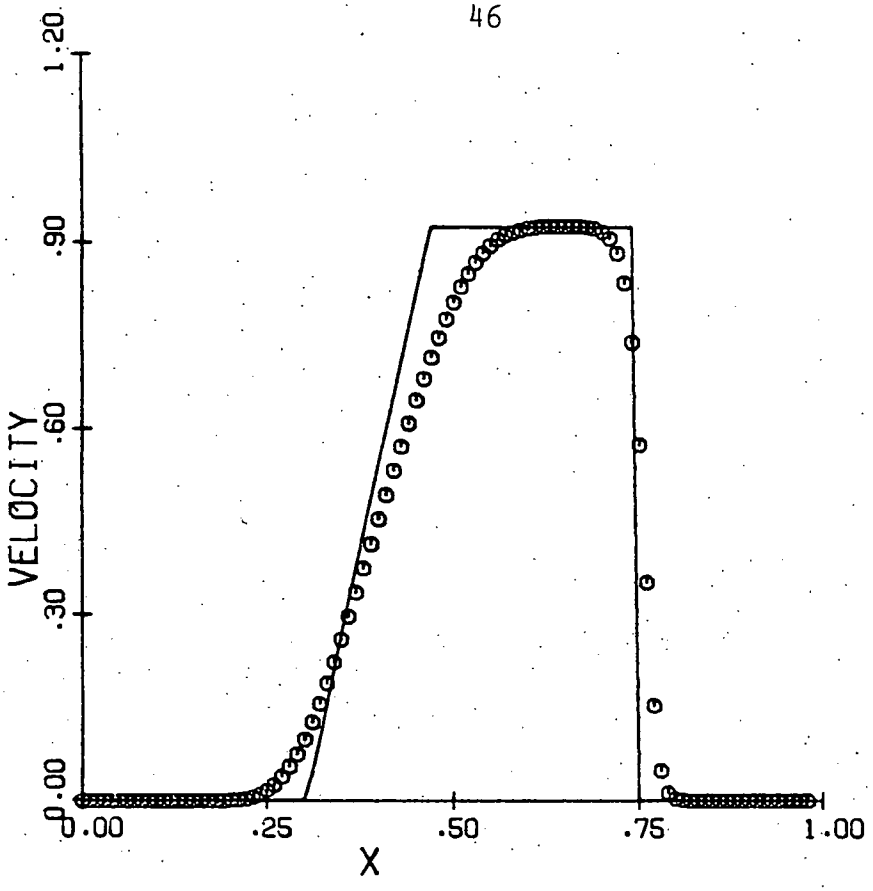

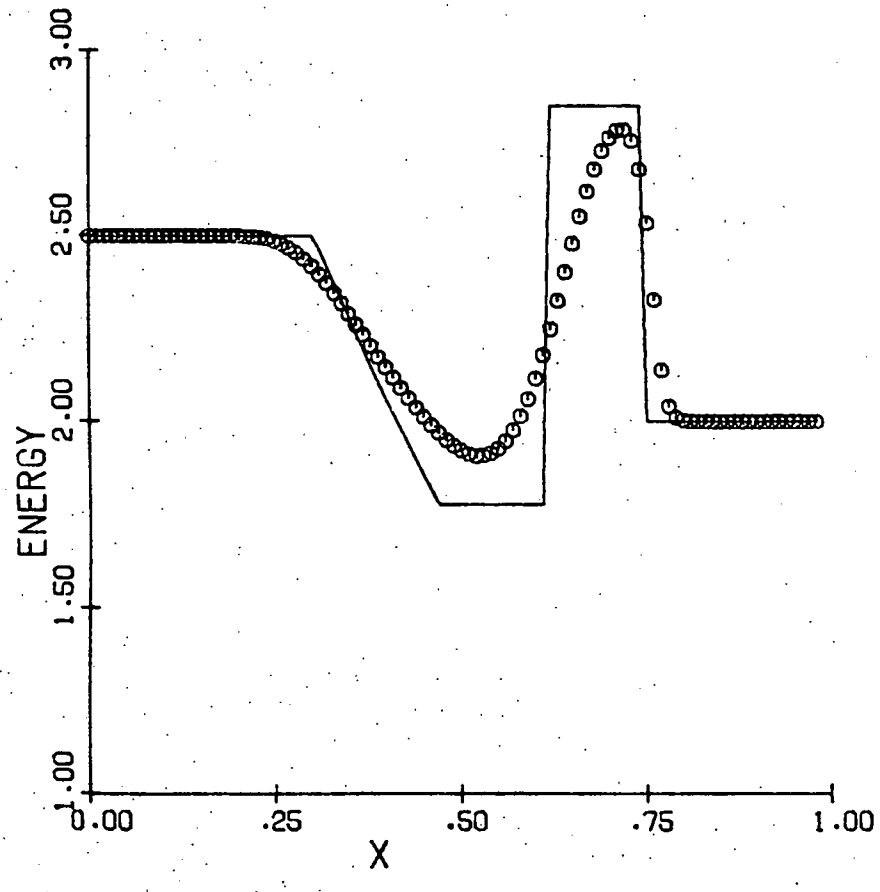

Figure 8 continued

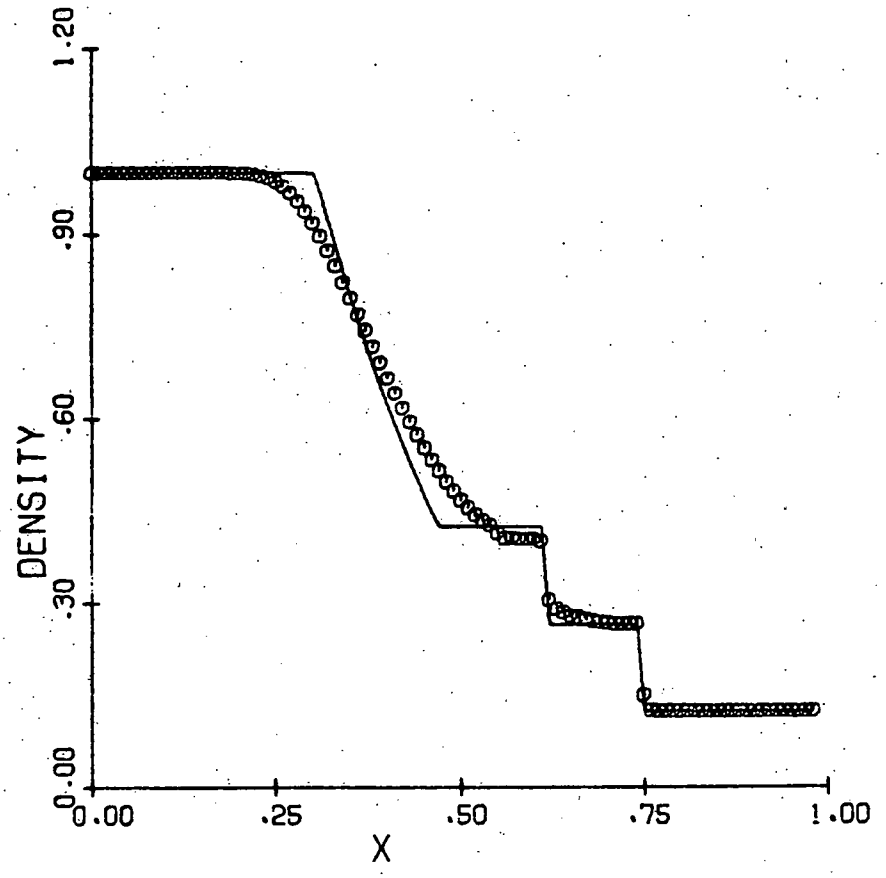
DENSITY
1.20
.90
.60
.30
0.00
0.00
.25
.50
.75
1.00
X

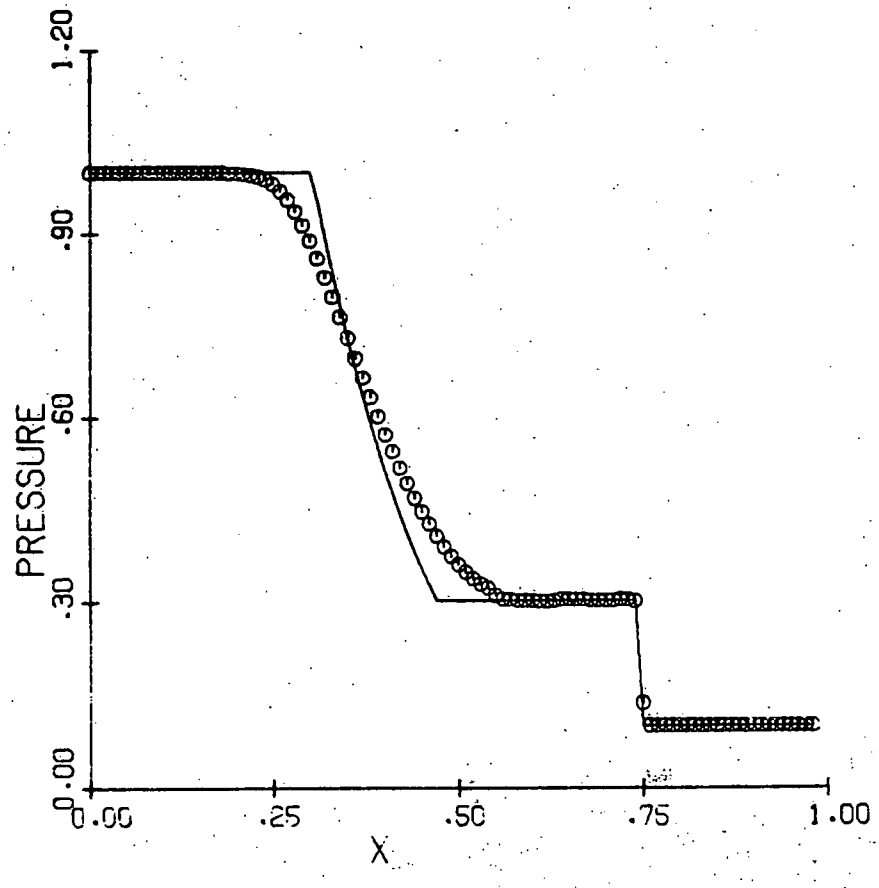
PRESSURE
1.20
.90
.60
.30
0.00
0.00
.25
.50
.75
1.00
X

Figure 9

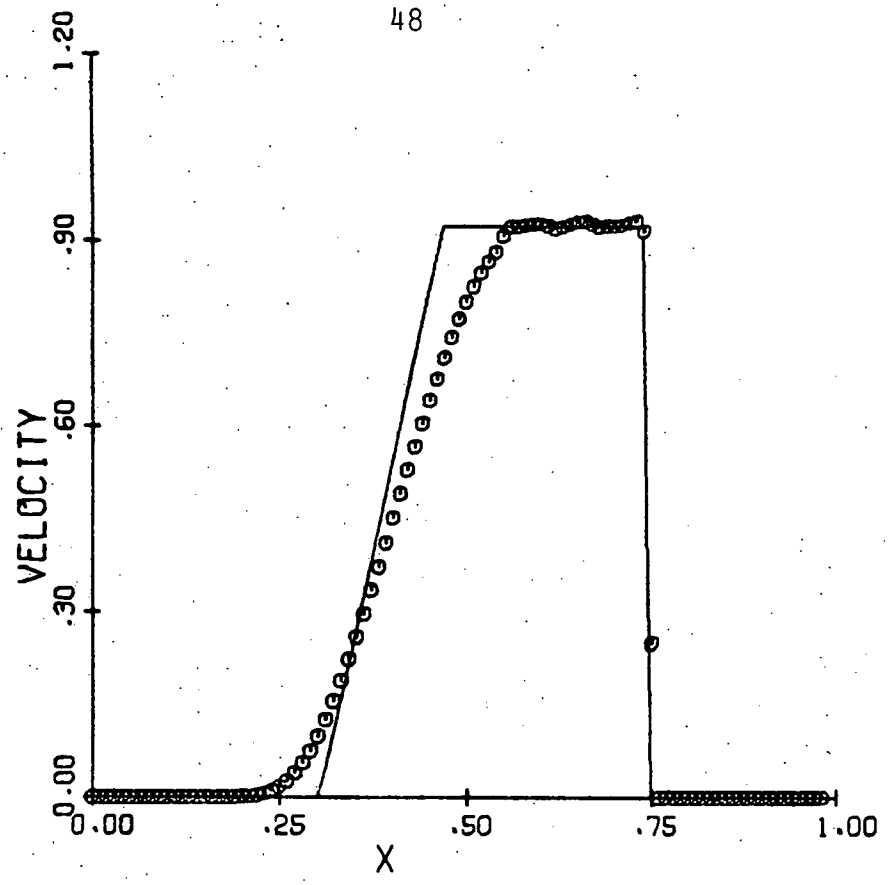

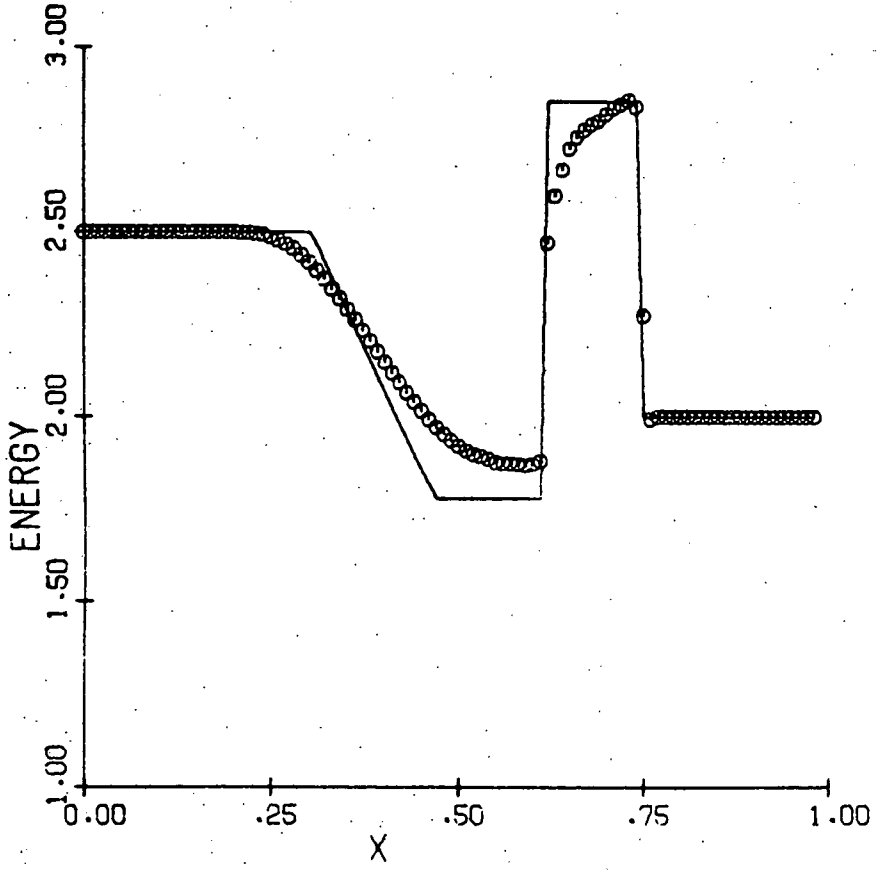

Figure 9 continued

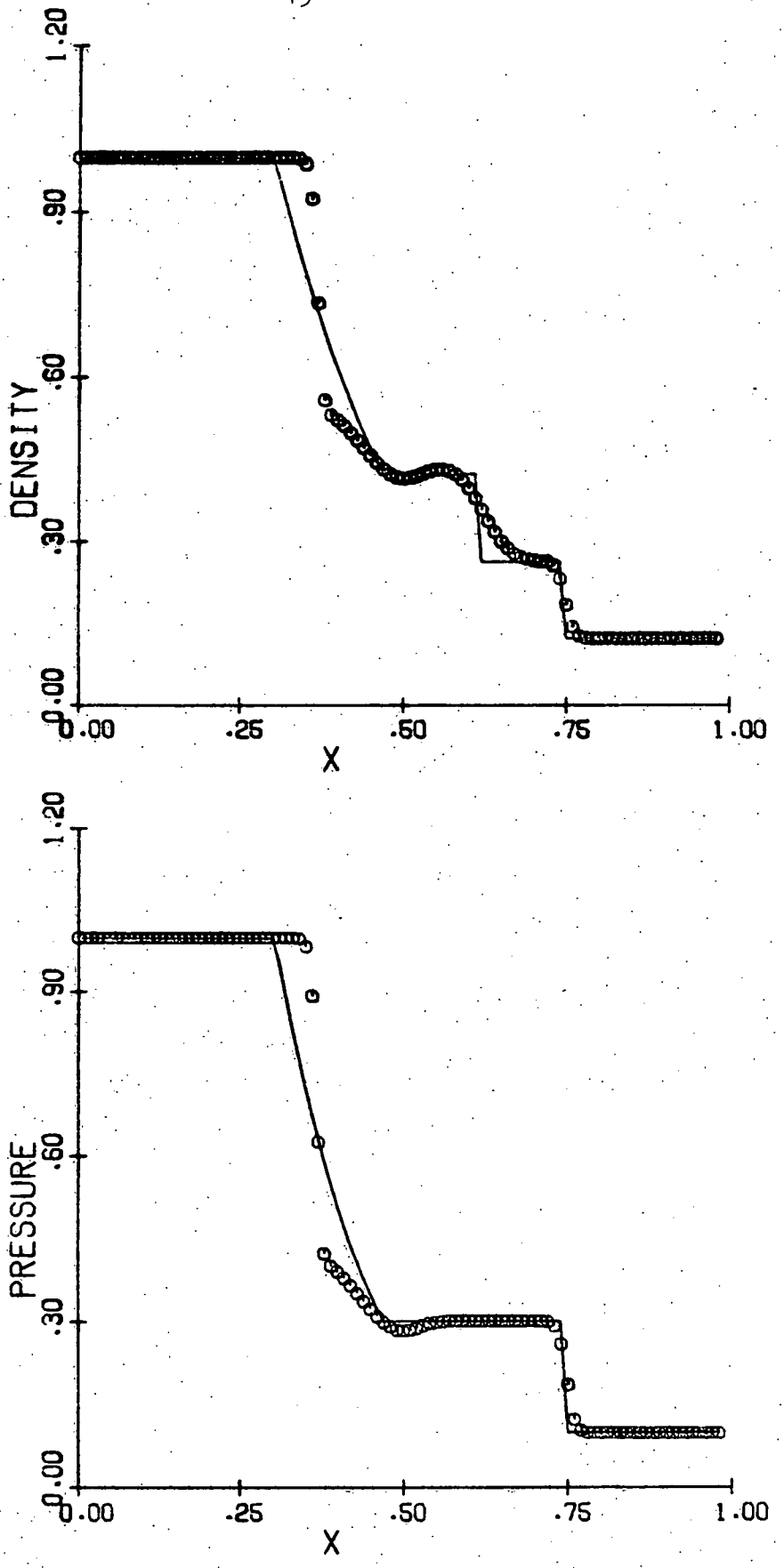
DENSITY
1.20
.90
.60
.30
0.00
0.00
.25
.50
.75
1.00
X
PRESSURE
1.20
.90
.60
.30
0.00
0.00
.25
.50
.75
1.00
X

Figure 10

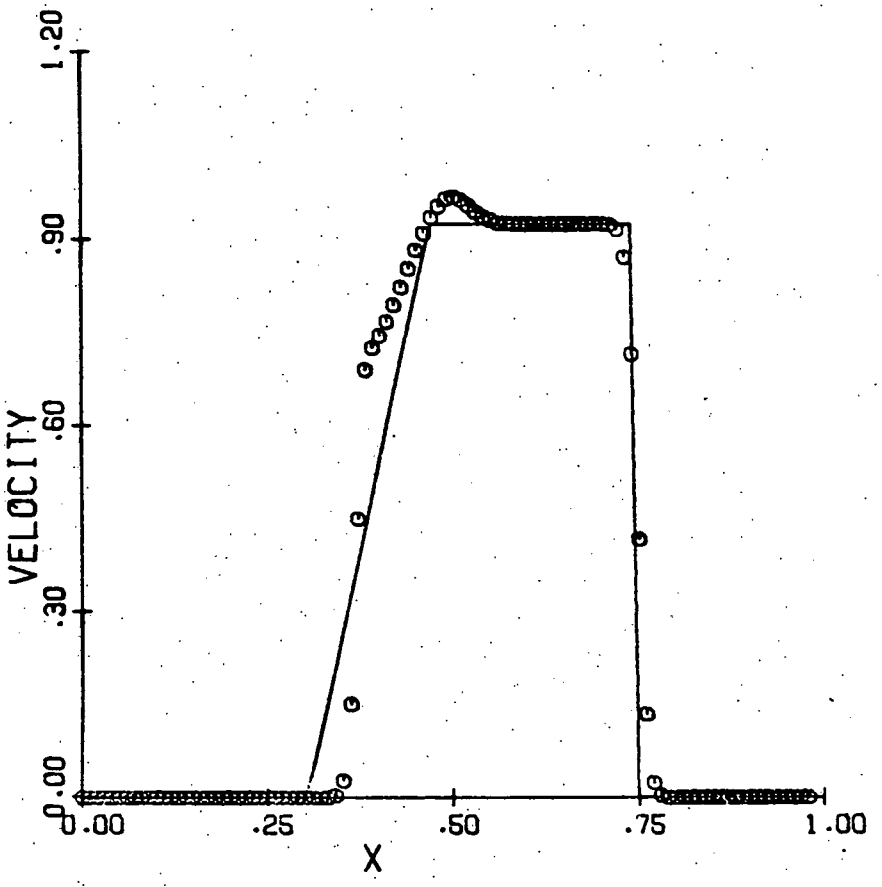

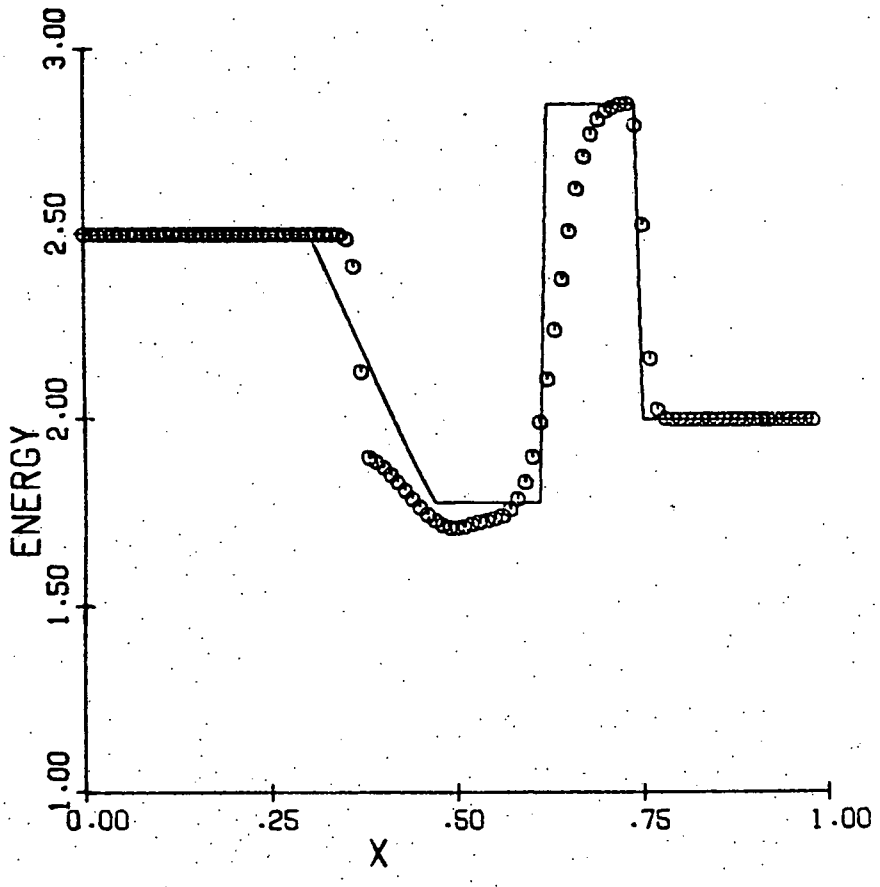

Figure 10 continued

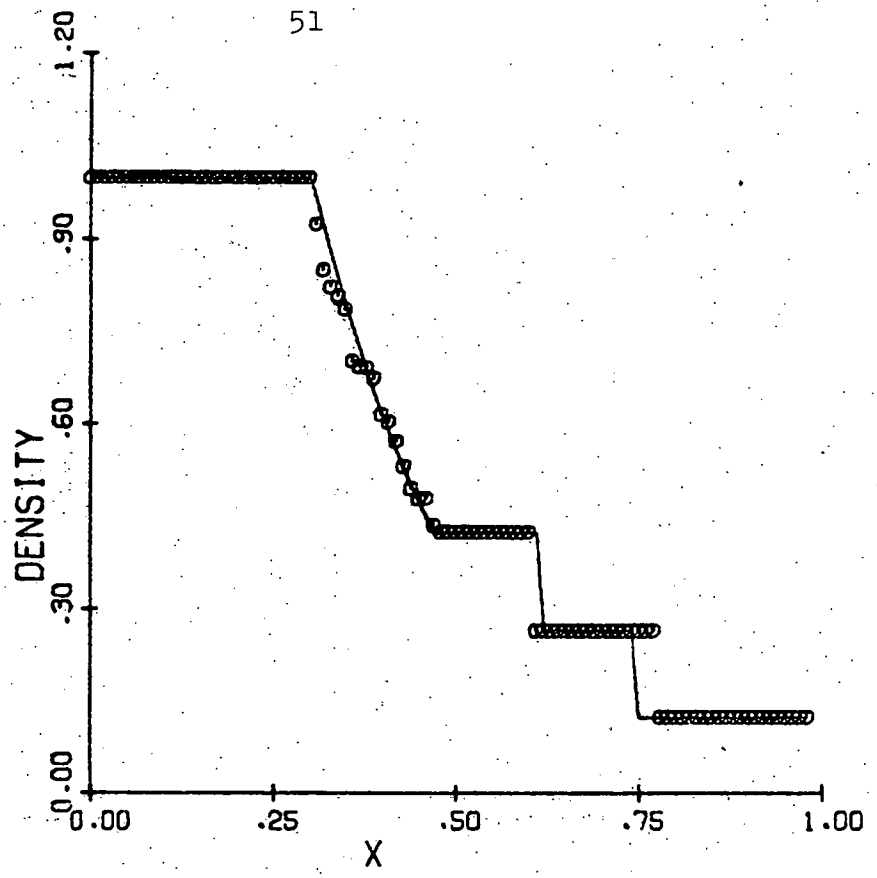
DENSITY
1.20
.90
.60
.30
0.00
0.00
.25
.50
.75
1.00
X

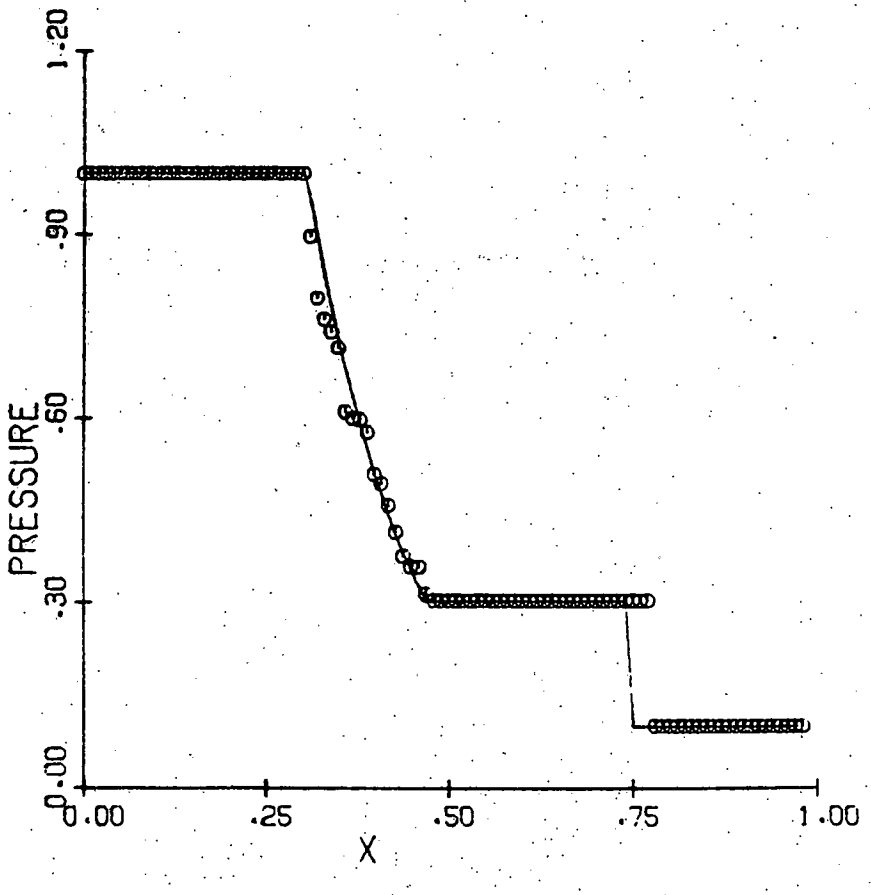
PRESSURE
1.20
.90
.60
.30
0.00
0.00
.25
.50
.75
1.00
X

Figure 11

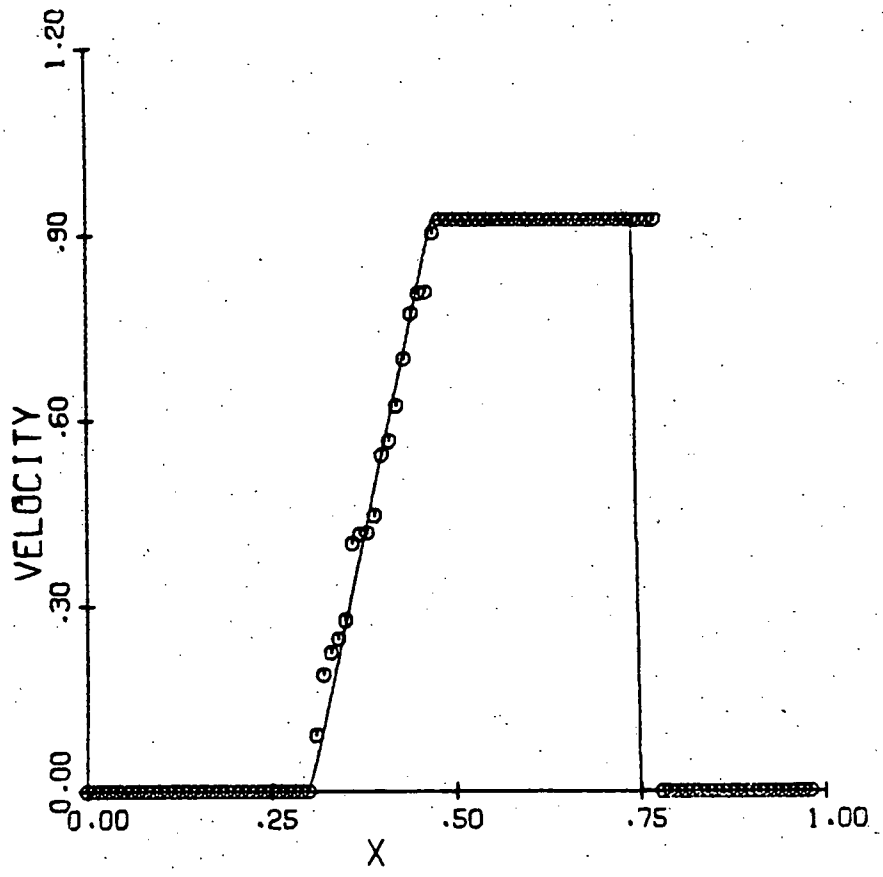

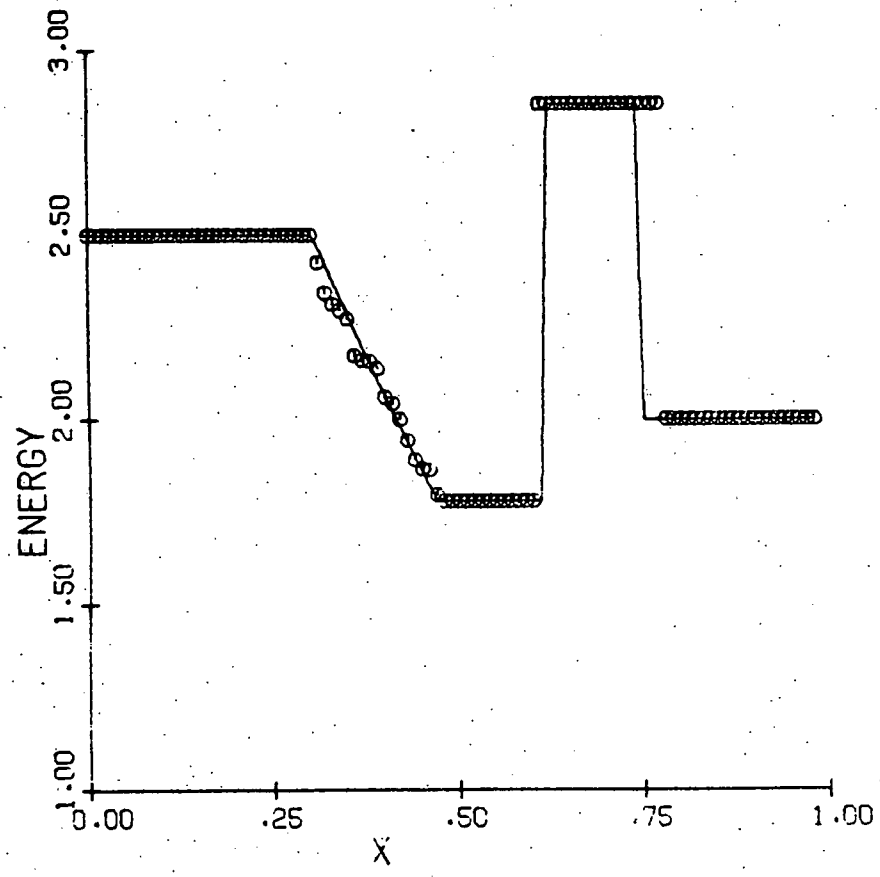

Figure 11 continued

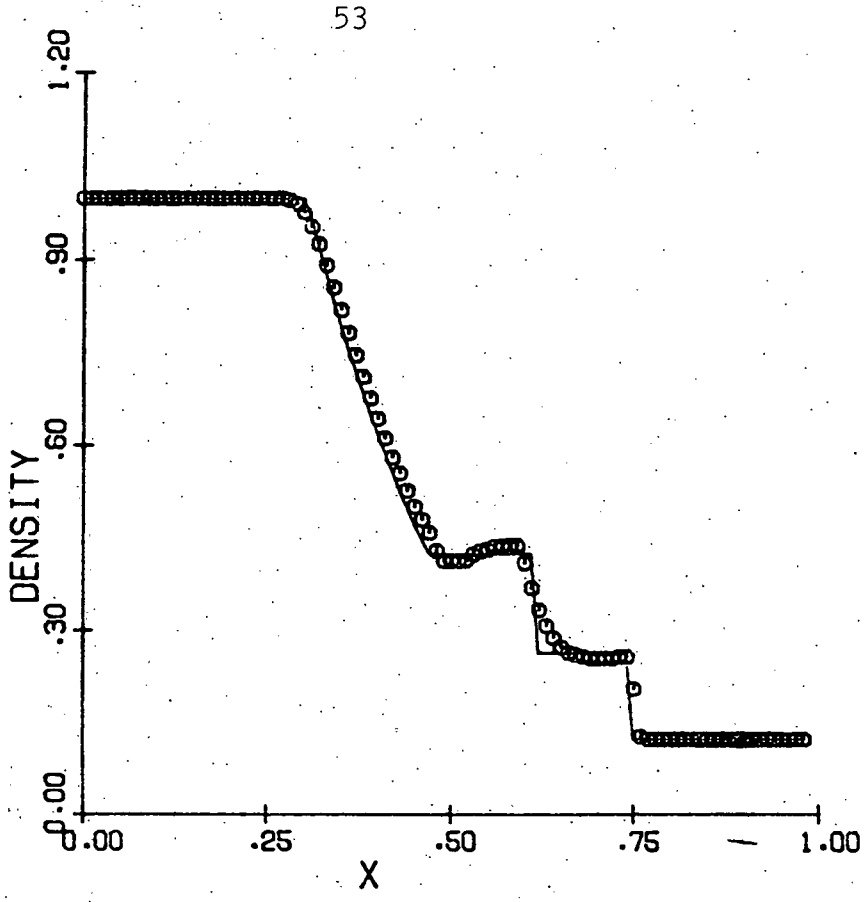
DENSITY
1.20
.90
.60
.30
0.00
0.00
.25
.50
.75
1.00
X

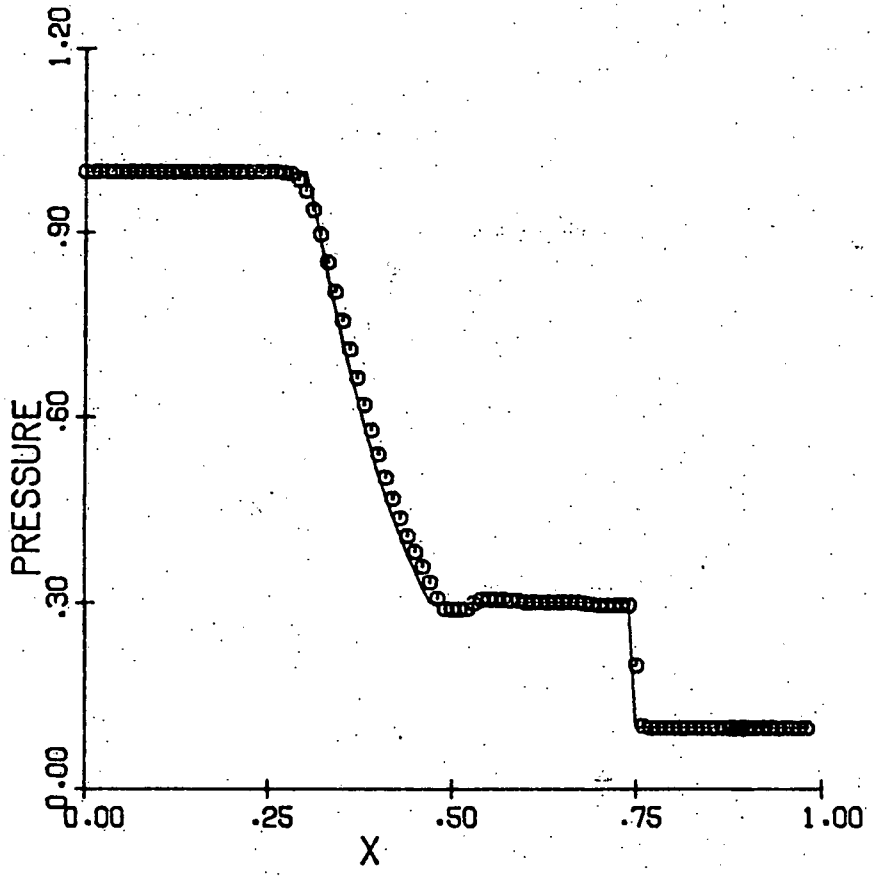
PRESSURE
1.20
.90
.60
.30
0.00
0.00
.25
.50
.75
1.00
X

Figure 12

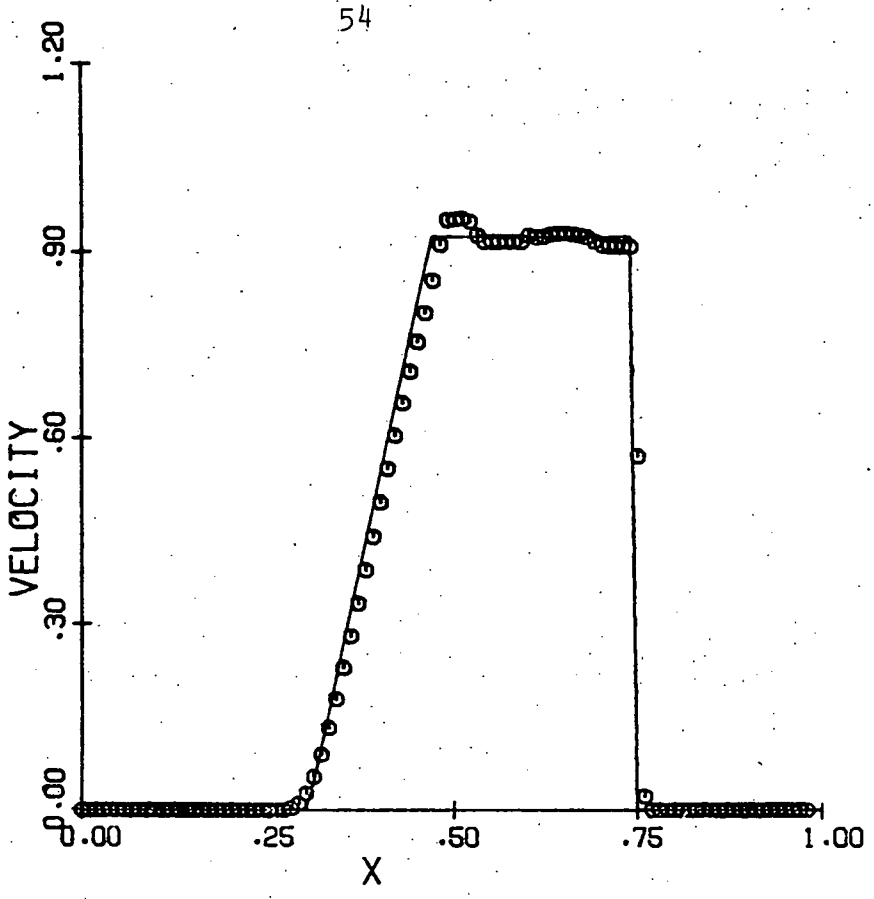

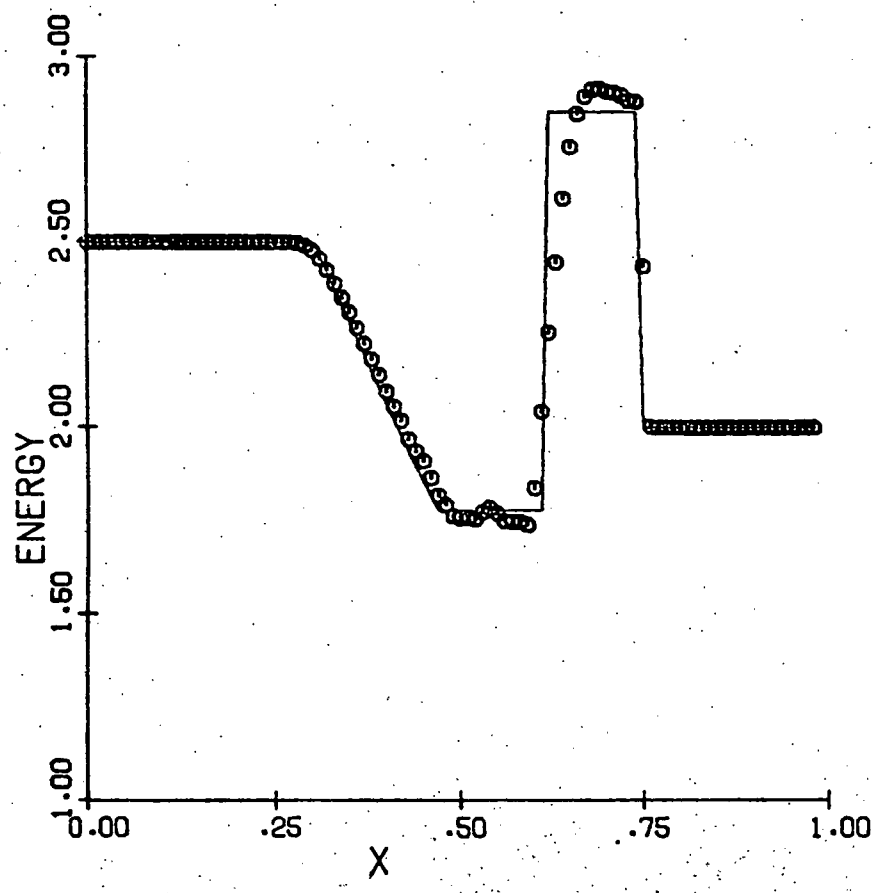

Figure 12 continued

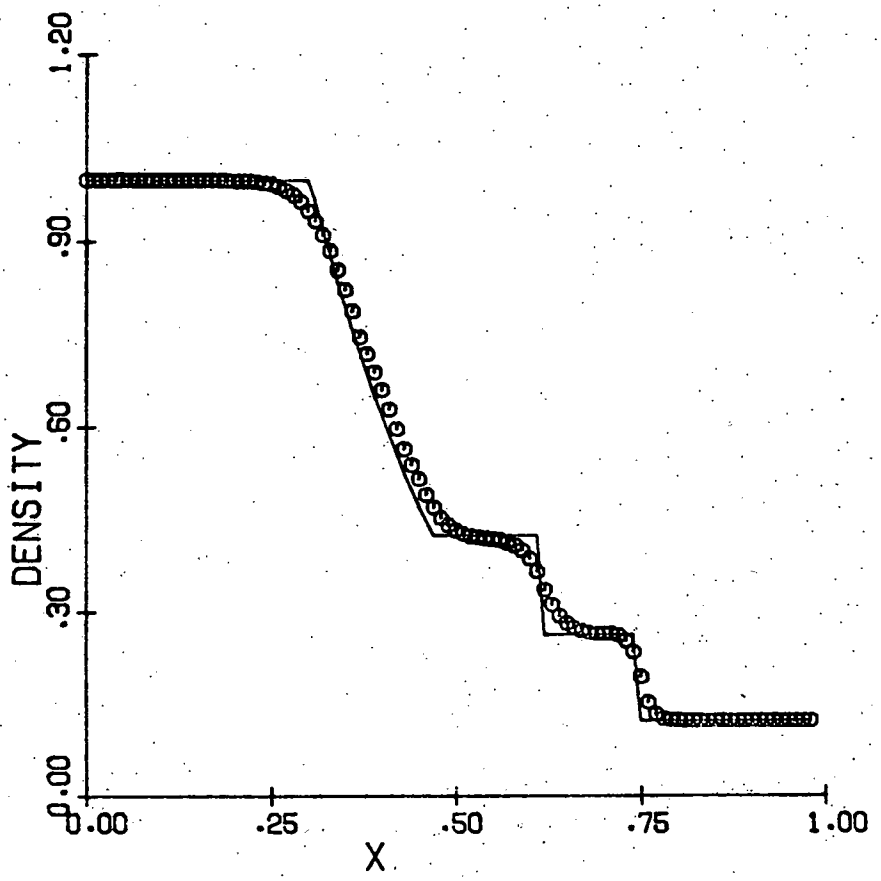
DENSITY
1.20
.90
.60
.30
0.00
0.00
.25
.50
.75
1.00
X

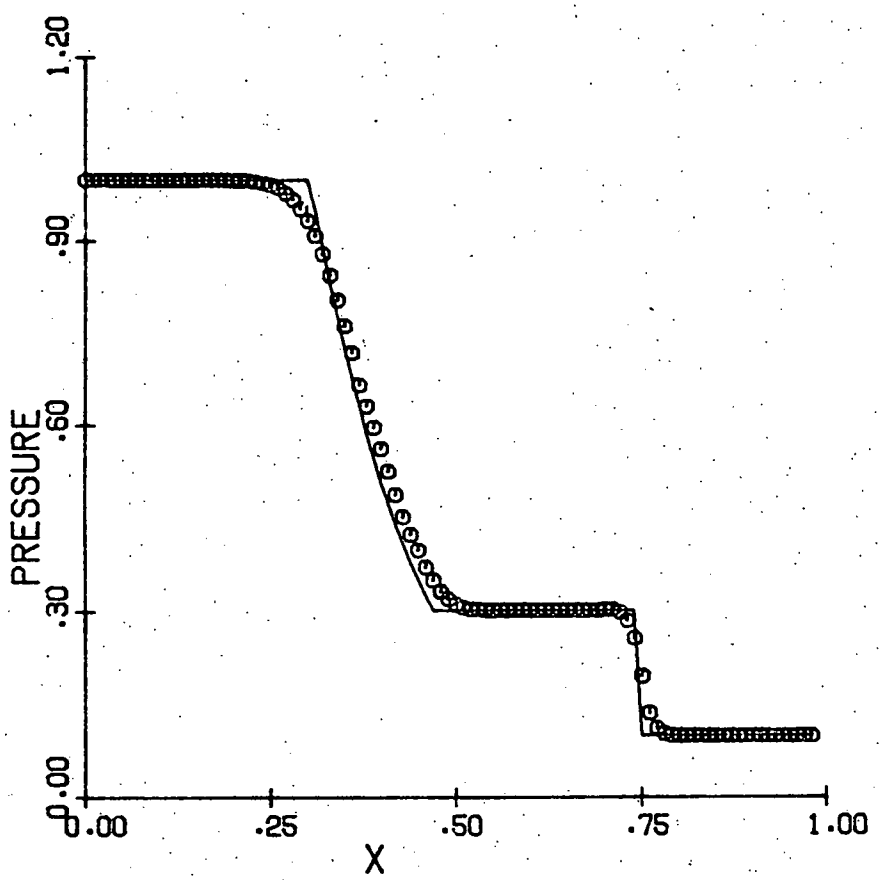
PRESSURE
1.20
.90
.60
.30
0.00
0.00
.25
.50
.75
1.00
X

Figure 13

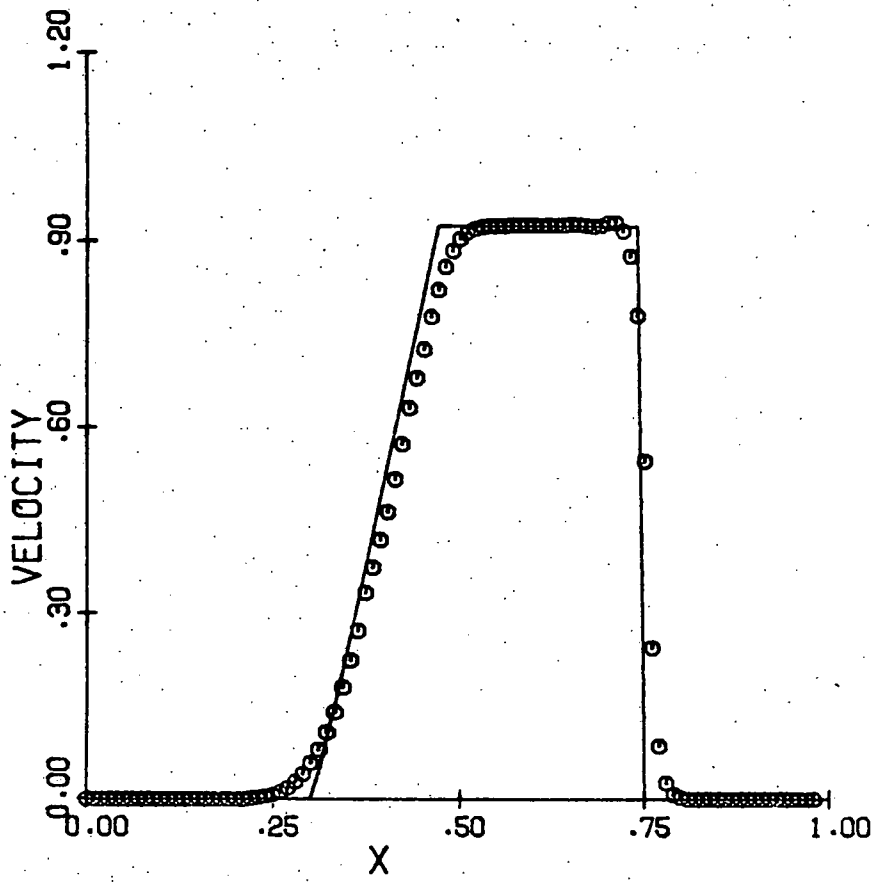

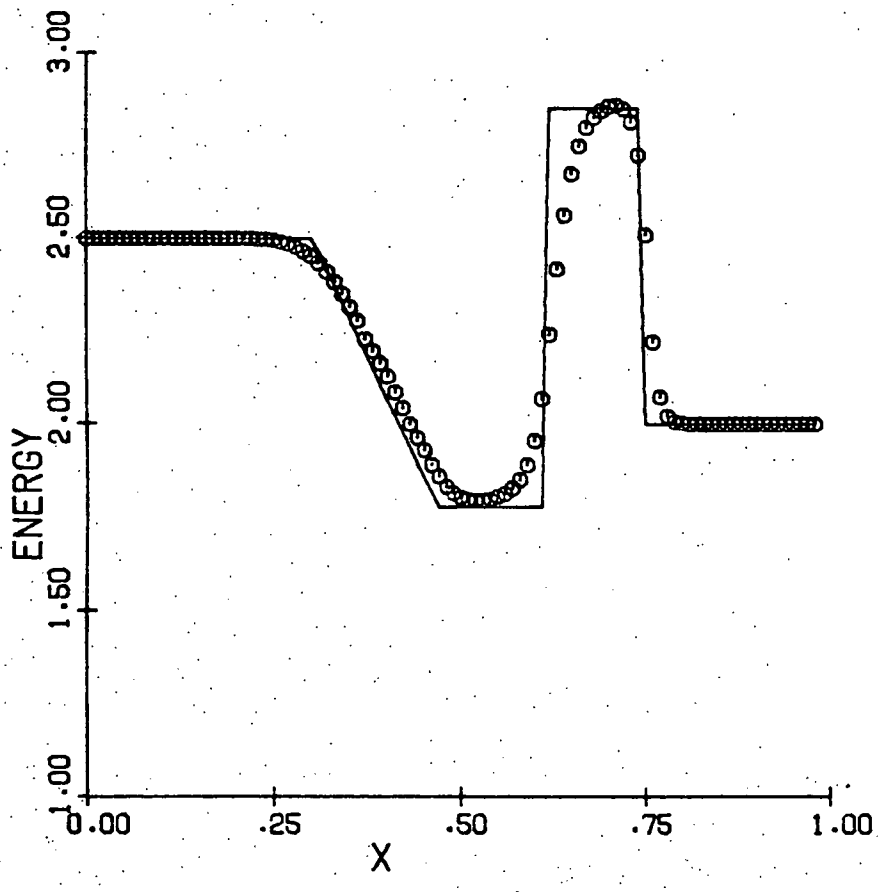

Figure 13 continued

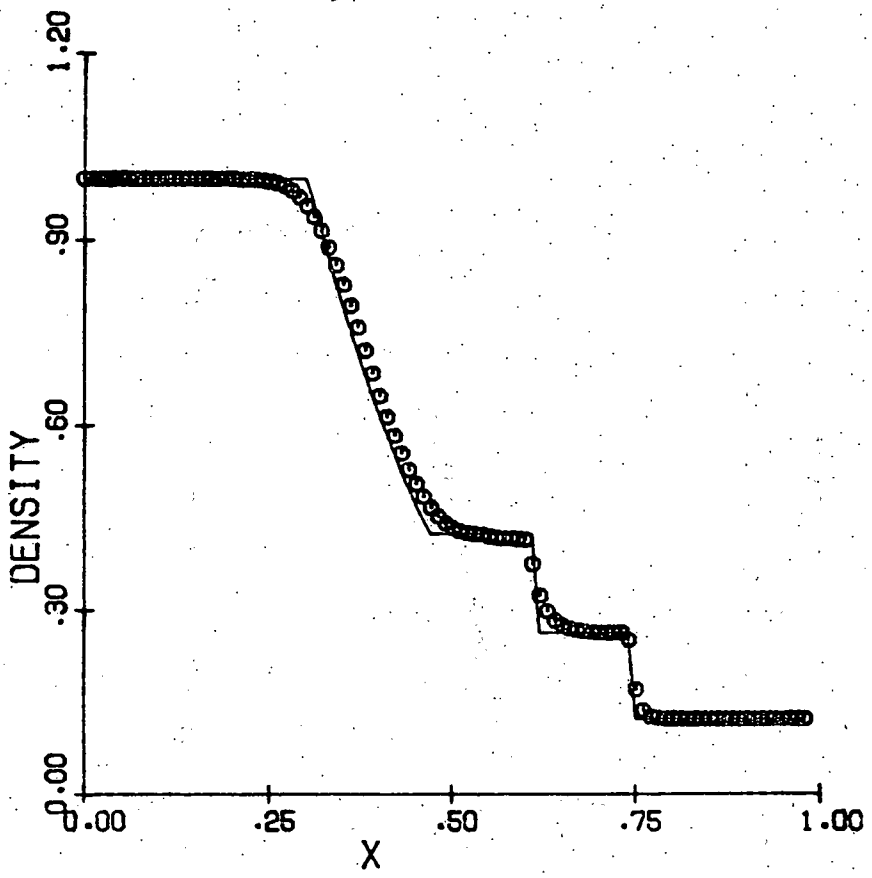
DENSITY
1.20
.90
.60
.30
0.00
0.00
.25
.50
.75
1.00
X

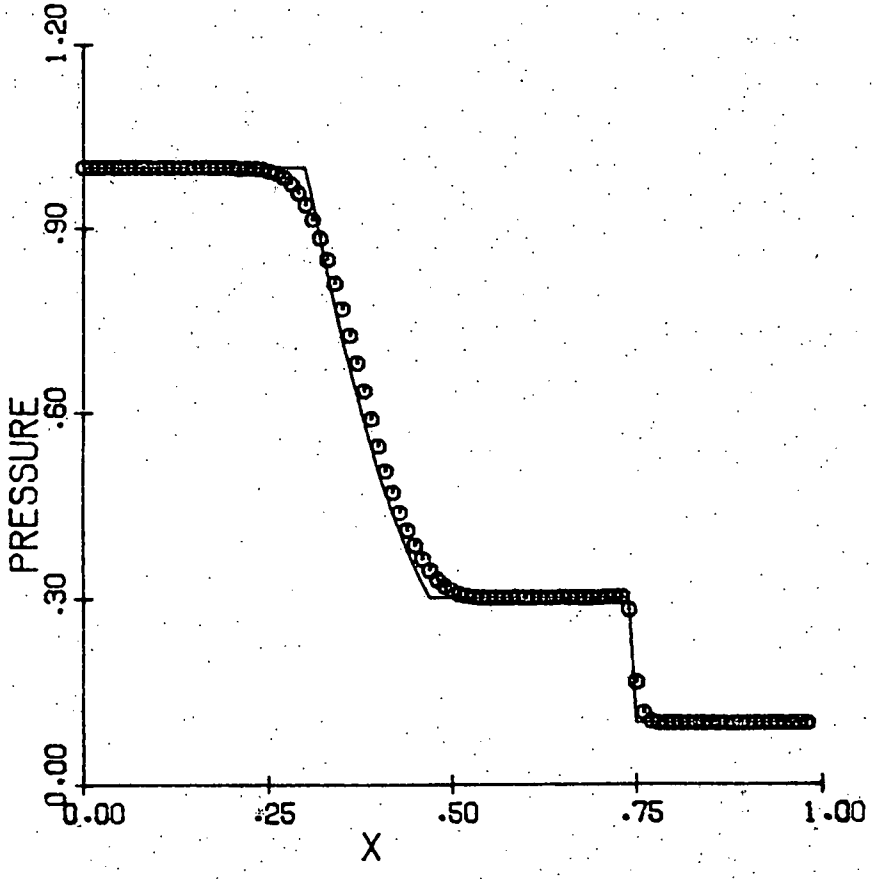
PRESSURE
1.20
.90
.60
.30
0.00
0.00
.25
.50
.75
1.00
X

Figure 14

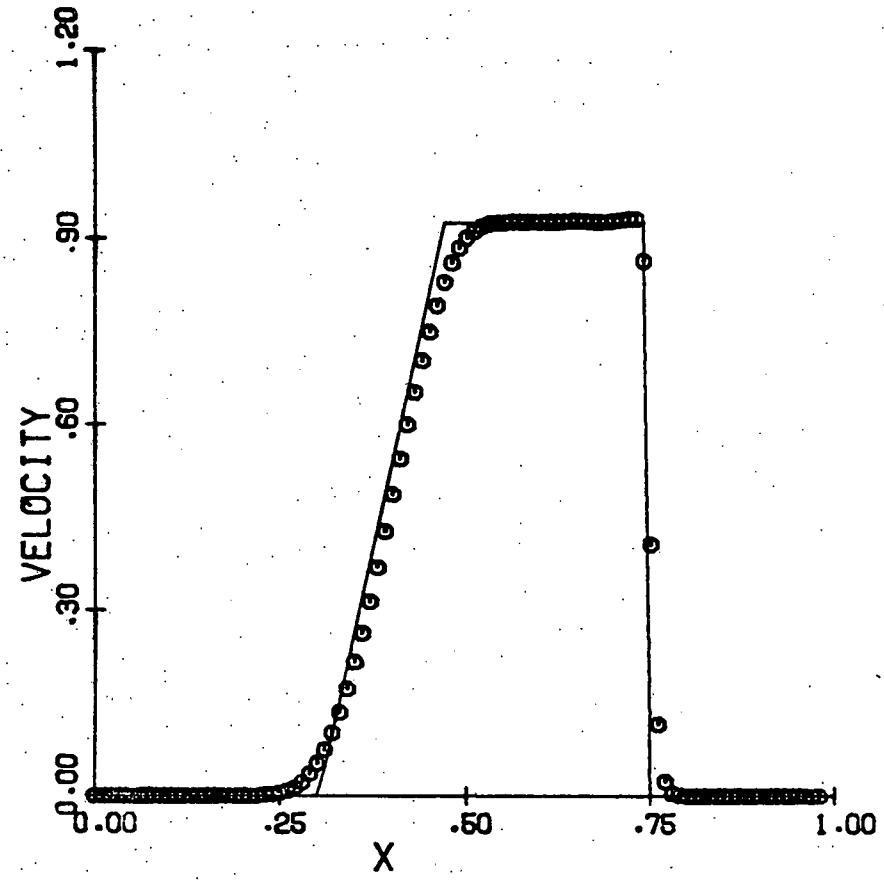

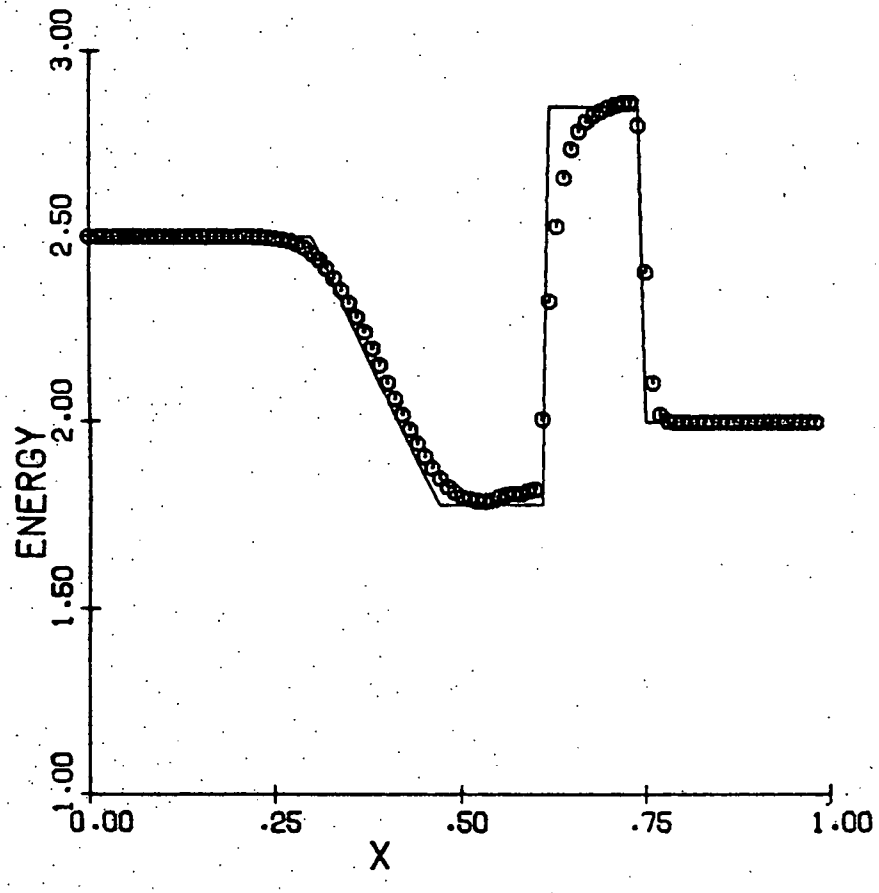

Figure 14 continued

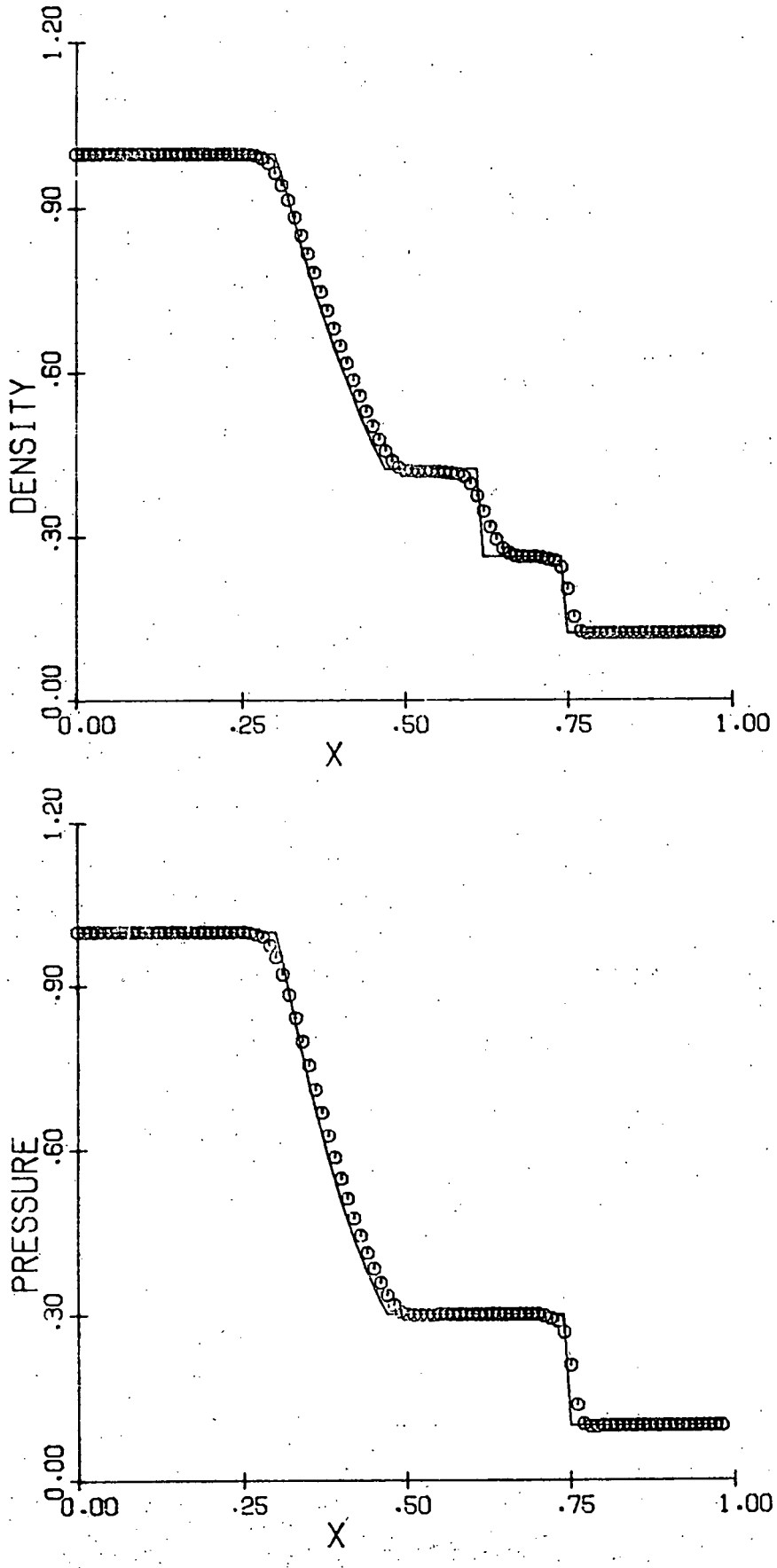
DENSITY
1.20
.90
.60
.30
0.00
0.00
.25
.50
.75
1.00
X
PRESSURE
1.20
.90
.60
.30
0.00
0.00
.25
.50
.75
1.00
X

Figure 15

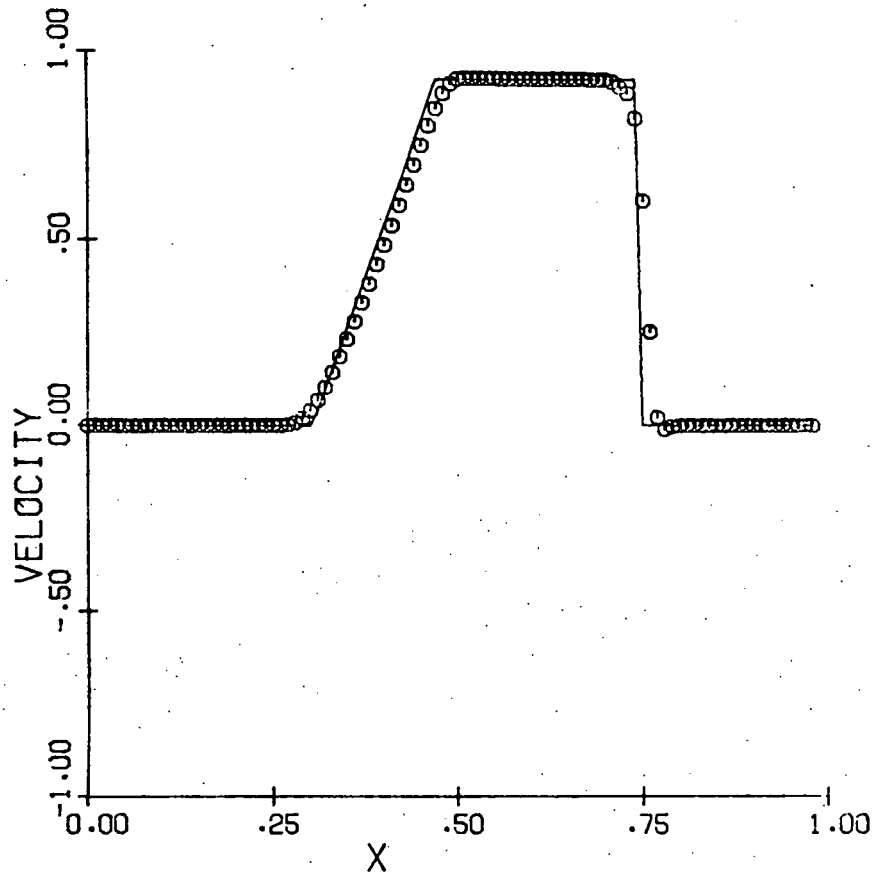

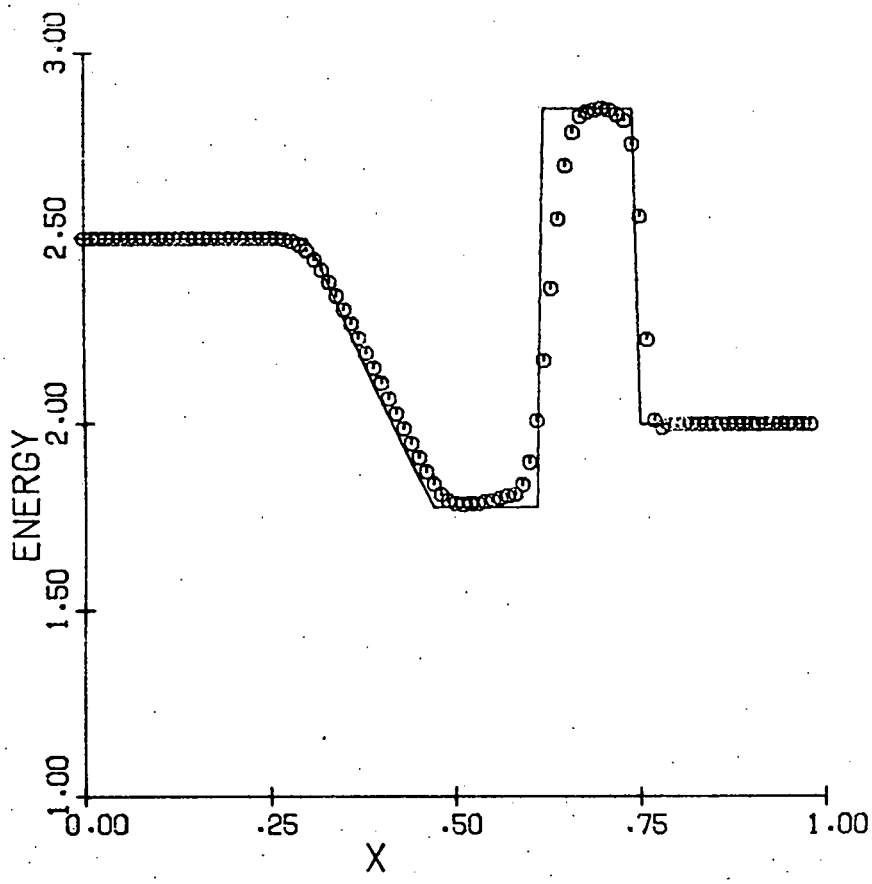

Figure 15 continued

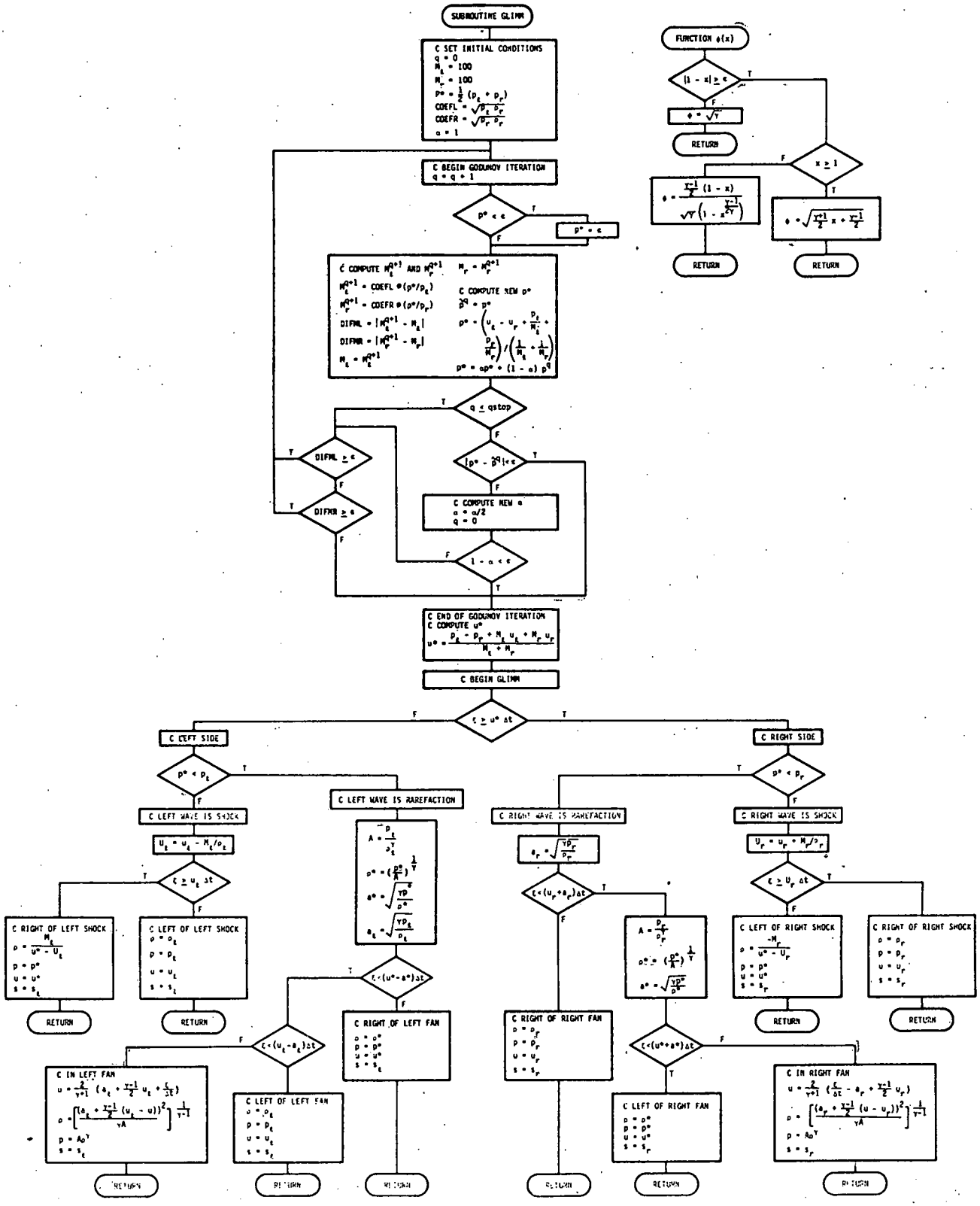
SUBROUTINE GLIMM
C SET INITIAL CONDITIONS
q = 0
M_ℓ = 100
M_r = 100
p* = ½ (p_ℓ + p_r)
COEFL = √(ρ_ℓ p_ℓ)
COEFR = √(ρ_r p_r)
a = 1
C BEGIN GODUNOV ITERATION
q = q + 1
p* < ε
p* = ε
C COMPUTE M_ℓ^{q+1} AND M_r^{q+1}
M_ℓ^{q+1} = COEFL ⊕ (p*/p_ℓ)
M_r^{q+1} = COEFR ⊕ (p*/p_r)
DIFML = |M_ℓ^{q+1} - M_ℓ|
DIFMR = |M_r^{q+1} - M_r|
M_ℓ = M_ℓ^{q+1}
M_r = M_r^{q+1}
C COMPUTE NEW p*
p^q = p*
p* = (u_ℓ - u_r + p_ℓ/M_ℓ + p_r/M_r) / (1/M_ℓ + 1/M_r)
p* = ap* + (1 - a) p^q
q ≤ qstop
DIFML ≥ ε
DIFMR ≥ ε
|p* - p^q| < ε
C COMPUTE NEW a
a = a/2
q = 0
1 - a < ε
C END OF GODUNOV ITERATION
C COMPUTE u*
u* = (p_ℓ - p_r + M_ℓ u_ℓ + M_r u_r) / (M_ℓ + M_r)
C BEGIN GLIMM
ξ ≥ u* Δt
C LEFT SIDE
p* < p_ℓ
C LEFT WAVE IS SHOCK
U_ℓ = u_ℓ - M_ℓ/ρ_ℓ
ξ ≥ U_ℓ Δt
C RIGHT OF LEFT SHOCK
ρ = M_ℓ/(u* - U_ℓ)
p = p*
u = u*
s = s_ℓ
RETURN
C LEFT OF LEFT SHOCK
ρ = ρ_ℓ
p = p_ℓ
u = u_ℓ
s = s_ℓ
RETURN
C LEFT WAVE IS RAREFACTION
A = p_ℓ/ρ_ℓ^γ
p* = (p*/A)^{1/γ}
a* = √(γp*/ρ*)
a_ℓ = √(γp_ℓ/ρ_ℓ)
ξ < (u* - a*) Δt
C RIGHT OF LEFT FAN
ρ = ρ*
p = p*
u = u*
s = s_ℓ
RETURN
ξ < (u_ℓ - a_ℓ) Δt
C IN LEFT FAN
u = 2/(γ+1) (a_ℓ + (γ-1)/2 u_ℓ + ξ/Δt)
ρ = [(a_ℓ + (γ-1)/2 (u_ℓ - u))^2 / γA]^{1/(γ-1)}
p = Aρ^γ
s = s_ℓ
RETURN
C LEFT OF LEFT FAN
ρ = ρ_ℓ
p = p_ℓ
u = u_ℓ
s = s_ℓ
RETURN
C RIGHT SIDE
p* < p_r
C RIGHT WAVE IS SHOCK
U_r = u_r + M_r/ρ_r
ξ ≥ U_r Δt
C LEFT OF RIGHT SHOCK
ρ = -M_r/(u* - U_r)
p = p*
u = u*
s = s_r
RETURN
C RIGHT OF RIGHT SHOCK
ρ = ρ_r
p = p_r
u = u_r
s = s_r
RETURN
C RIGHT WAVE IS RAREFACTION
a_r = √(γp_r/ρ_r)
ξ < (u_r + a_r) Δt
A = p_r/ρ_r^γ
p* = (p*/A)^{1/γ}
a* = √(γp*/ρ*)
C RIGHT OF RIGHT FAN
ρ = ρ_r
p = p_r
u = u_r
s = s_r
RETURN
ξ < (u* + a*) Δt
C LEFT OF RIGHT FAN
ρ = ρ*
p = p*
u = u*
s = s_r
RETURN
C IN RIGHT FAN
u = 2/(γ+1) (ξ/Δt - a_r + (γ-1)/2 u_r)
ρ = [(a_r + (γ-1)/2 (u - u_r))^2 / γA]^{1/(γ-1)}
p = Aρ^γ
s = s_r
RETURN
FUNCTION φ(x)
|1 - x| ≥ ε
φ = √γ
RETURN
x ≥ 1
φ = (γ+1)/2 (1 - x) / √γ (1 - x^{(γ-1)/2γ})
RETURN
φ = √((γ+1)/2 x + (γ-1)/2)
RETURN

Figure 16

List of Captions

Tables.

Figures.

Bibliography

[1] J. P. Boris and D. L. Book, J. Comp. Phys. 11, 38 (1973).

[2] _____, and K. J. Hain, J. Comp. Phys. 18, 248 (1975).

[3] A. J. Chorin, J. Comp. Phys. 22, 517 (1976).

[4] S. K. Godunov, Mat. Sbornik, 47, 271 (1959).

[5] _____, A. V. Zabrodin, and G. P. Prokopov, J. Comp. Math. Math. Phys., USSR, 1, 1187 (1962).

[6] J. Glimm, Comm. Pure Appl. Math., 18, 697 (1965).

[7] A. Harten, The Method of Artificial Compression, AEC Research and Development Report C00-3077-50, New York University (1974).

[8] _____, The Artificial Compression Method for Shocks and Contact Discontinuities: I Single Conservation Laws, Comm. Pure Appl. Math., to appear.

[9] _____, The Artificial Compression Method for Shocks and Contact Discontinuities: III Self-Adjusting Hybrid Schemes, to appear.

[10] _____ and G. Sod, A Generalized Version of Glimm's Method, to appear.

[11] _____ and G. Zwas, J. Comp. Phys., 6, 568 (1972).

[12] J. M. Hyman, On Robust and Accurate Methods for the Calculation of Compressible Fluid Flows I, to appear.

[13] A. Lapidus, J. Comp. Phys., 2, 154 (1967).

[14] P. D. Lax, Comm. Pure Appl. Math., 7, 159 (1954).

[15] _____, Comm. Pure Appl. Math., 10, 537 (1957).

[16] _____ and B. Wendroff, Comm. Pure Appl. Math., 13, 217 (1960).

[17] B. van Leer, J. Comp. Phys., 3, 473 (1969).

[18] R. MacCormack, Proceedings of the Second International Conference on Numerical Methods in Fluid Dynamics, Lecture Notes in Physics, Vol. 8, ed. M. Holt, Springer-Verlag, New York (1971).

[19] R. Richtmyer and K. Morton, Difference Methods for Initial-Value Problems, 2nd ed., Interscience (1967).

[20] V. V. Rusanov, J. Comp. Math. Math. Phys., USSR, No. 2 (1962).

[21] G. A. Sod, The Computer Implementation of Glimm's Method, UCID-17252, Lawrence Livermore Laboratory, University of California (1976).

[22] _____, A Numerical Study of a Converging Cylindrical Shock, J. Fluid Mech., to appear. Also ERDA Research and Development Report C00-3077-144, New York University (1977).